iScience

CellPress
OPEN ACCESS

Article

Intrauterine desensitization enables long term survival of human oligodendrocyte progenitor cells without immunosuppression

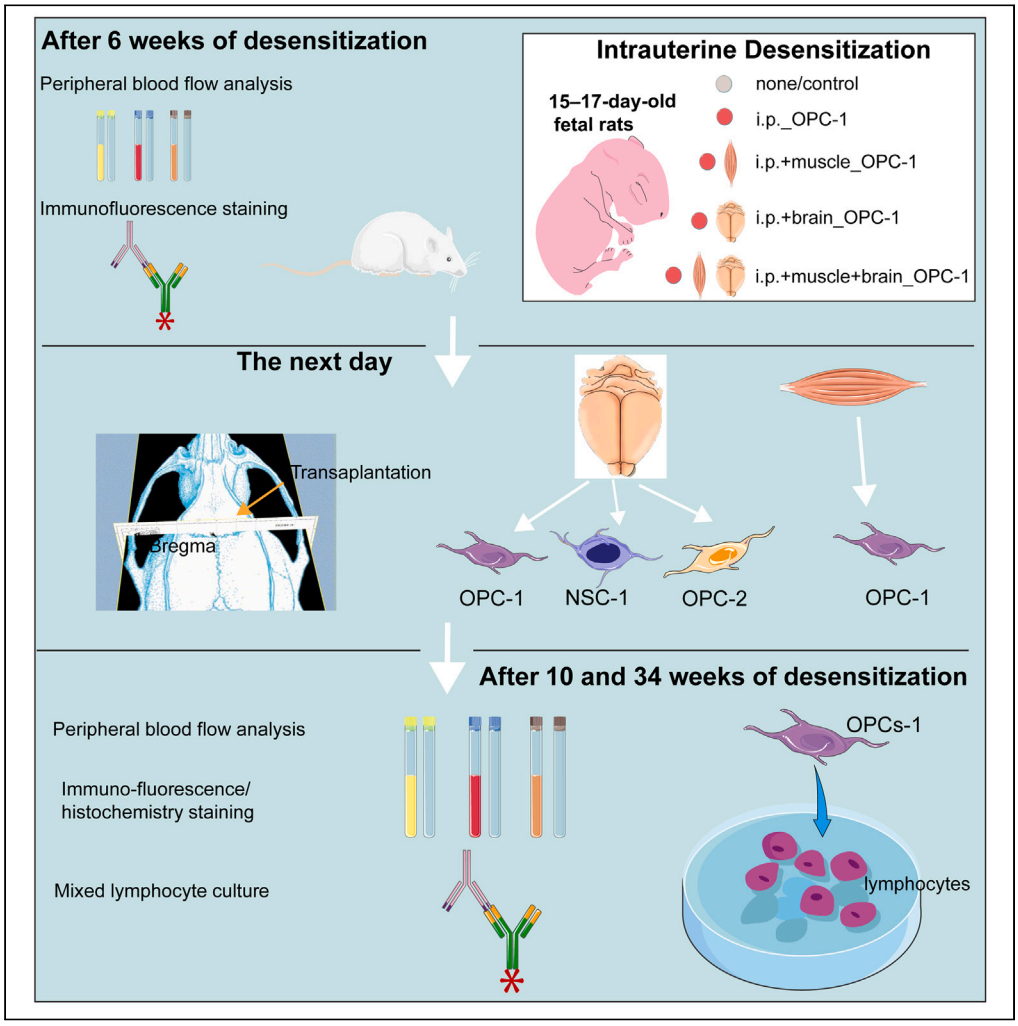

Dou Ye, Suqing Qu, Yinxiang Yang, ..., Ruiqin Yao, Zhichun Feng, Zuo Luan

wenxi_yao@163.com (R.Y.)
byfengzc@163.com (Z.F.)
luanzuo@aliyun.com (Z.L.)

Highlights

Desensitization enabled desensitized cells survival in the center and periphery

Desensitization reduced the inflammatory response to transplantation

Central nervous system is in a relatively tolerance to transplantation

This study guides the immune tolerance through desensitization in preterm infants

Ye et al., iScience 26, 106647
May 19, 2023
https://doi.org/10.1016/j.isci.2023.106647

iScience

CellPress
OPEN ACCESS

Article

Intrauterine desensitization enables long term survival of human oligodendrocyte progenitor cells without immunosuppression

Dou Ye,[1,2,6,7] Suqing Qu,[1,6] Yinxiang Yang,[1] Zhaoyan Wang,[1] Qian Wang,[1] Weipeng Liu,[1] Fan Zhang,[1,2] Qian Guan,[1] Xiaohua Wang,[1] Jing Zang,[1] Xin Li,[1] Hengtao Liu,[3] Ruiqin Yao,[4,*] Zhichun Feng,[5,*] and Zuo Luan[1,2,*]

SUMMARY

Immune rejection can be reduced using immunosuppressants which are not viable for premature infants. However, desensitization can induce immune tolerance for premature infants because of underdeveloped immune system. The fetuses of Wistar rats at 15–17 days gestation were injected via hOPCs-1 into brain, muscles, and abdomen ex utero and then returned while the fetuses of control without injection. After 6 weeks of desensitization, the brain and muscles were transplanted with hOPCs-1, hNSCs-1, and hOPCs-2. After 10 and 34 weeks of desensitization, hOPCs-1 and hNSCs-1 in desensitized groups was higher than that in the control group while hOPCs-2 were rejected. Treg, CD4CD28, CD8CD28, and CD45RC between the desensitization and the control group differed significantly. Inflammatory cells in group with hOPCs-1 and hNSCs-1 was lower than that in the control group. hOPCs-1 can differentiate into myelin in desensitized groups. Wistar rats with desensitization developed immune tolerance to desensitized and transplanted cells.

INTRODUCTION

Premature infants with white matter injury (WMI) are often associated with neurodevelopmental sequelae such as cognitive and behavioral disorders, and cerebral palsy with the pathophysiologic characteristics associated with poor myelination, and a global health concern and the most common cause of chronic neurological morbidity.[1] Since clinically effective treatments are currently unavailable, exploring effective treatments for premature white matter injury (PWMI) is necessary.[2] Endogenous oligodendrocyte precursor cells (OPCs) may promote re-myelination in acute demyelinating lesions but not myelination in chronic demyelinating lesions.[3] Despite numerous intact-appearing axons, newly generated endogenous OPCs fail to differentiate and initiate myelination along their normal developmental trajectory in preterm infants with WMI.[4] Therefore, transplantation of exogenous hOPCs is a promising therapeutic option for WMI in premature infants.[5] Transplantation of exogenous hOPCs can effectively promote myelin repair.[6] For example, transplanting hOPCs into neonatal Shiverer mice can promote cerebral myelination in congenital demyelination[7]; embryonic stem cell (ESC)-derived OLs transplanted into Sprague-Dawley (SD) rats can migrate into white matter and repair white matter structure and function[8]; transplantation of hOPCs restored neurobehavioral functions by preventing axonal demyelination in SD rats.[9] hOPCs can be used in the cell therapy of perinatal hypoxic-ischemic and infectious brain injuries, including periventricular leukomalacia and cerebral palsy.[10] Therefore, overcoming the immune rejection of exogenous hOPC transplantation is a problem faced by both researchers and clinicians.

Researchers have tried to solve this using numerous methods, including donor matching and graft and recipient preconditioning (myeloablative therapy, plasma exchange, splenectomy, and immunosuppressants).[11] These treatments against graft rejection may predispose the recipients to side effects e.g., endangering both life quality and expectancy.[12] The satisfactory strategy is to induce low responsiveness or irresponsiveness in recipients of donor grafts while preserving the normal immunological functions in antigen recognition and infection prevention. This way, successful transplantation strategies include weakening the immune response or inducing immune tolerance to the grafts[13] based on abstinence clones. Moreover, the immature immune development in premature infants can be used to create abstinence clones, where the lymphocyte clones are damaged and inhibited when they encounter internal antigens or are artificially

[1]Department of Pediatrics, the Sixth Medical Centre, Chinese PLA General Hospital, Beijing 100037, China

[2]Medical School of Chinese PLA, Beijing 100853, China

[3]Jiaen Genetics Laboratory, Beijing Jiaen Hospital, Beijing 100191, China

[4]Department of Neurobiology, Xuzhou Key Laboratory of Neurobiology, Xuzhou Medical University, Xuzhou, Jiangsu Province 221004, China

[5]Faculty of Pediatrics, The Seventh Medical Centre, Chinese PLA General Hospital, 100700 Beijing, China

[6]These authors contributed equally

[7]Lead contact

*Correspondence: wenxi_yao@163.com (R.Y.), byfengzc@163.com (Z.F.), luanzuo@aliyun.com (Z.L.)

https://doi.org/10.1016/j.isci.2023.106647

introduced to foreign antigens during the embryonic stage. In postnatal life, abstinence clones remain inactive to internal antigens or the artificially introduced foreign antigens present *in utero*, indicating that adults can form immunologic tolerance to antigens prior to exposure during the embryonic period.[13,14] White matter damage is common in preterm fetuses aged 28–32 weeks.[15] At this stage, immune development is incomplete,[16] and the development of T regulatory (Treg) peaks that facilitates the induction of immune tolerance.[17,18] Therefore, we desensitized premature infants via hOPCs transplantation to induce immune tolerance.

In this study, we transplanted hOPCs-1 into the abdomen, brain, and muscles (the left forelimbs) of 15–17-day-old fetal rats (desensitization) to explore the difference in immune tolerance induced by central and peripheral desensitization. After six weeks of desensitization, the rats were transplanted with the hOPCs-1, hNSCs-1, and hOPCs-2 in the brain, and the desensitized (the left forelimbs) and un-desensitized (the right hind limbs) muscles (transplantation). We also observed the changes in Treg, CD4CD28, CD8CD28, and CD45RC in the peripheral blood of six-, 10-, and 34-week-old rats to explore their immune response to grafts. Finally, we observed the survival, differentiation, and local inflammatory response of transplanted cells via immunofluorescence staining of Stem121, human nuclear antigen (HNA), and myelin basic protein (MBP) and immunohistochemical staining of CD4, CD8, and OX42 in the desensitized and near the corpus callosum, respectively.

RESULTS

Characterization of hOPCs and hNSCs

Oligodendrocyte progenitor cell bodies are fully round or spindle-shaped with strong refraction, and protrusions are bipolar bead-like, elongated, or have more than two poles (Figure 1A). Flow cytometric analysis of hOPCs showed that the positive rates of A2B5, PDGFR-a, OLIG2, and SOX10 were 48.3, 82.0, 95.6, and 92.4%, respectively (Figure 1B). The immunofluorescence staining results of hOPCs showed that A2B5, PDGFR-α, OLIG2, and SOX10 were positive (Figure 1C). hNSCs were cultured as a suspended state of neuro-spheres, had a good refractive index, and exhibited minute protrusions around the spheroids; the sizes of the neuro-spheres varied, with an average diameter of 200–250 μm (Figure 1D). Immunofluorescence staining showed a positive result for the NSC-specific antigen, nestin (Figure 1D).

Survival of hOPCs after transplantation in intrauterine desensitized rats and differentiation

Six weeks after intrauterine desensitization (Table 1), we traced the hOPCs in the rat brain and muscle using immunofluorescence staining and revealed that Stem121 was positive in the desensitization sites (Figure 2A). Six weeks after desensitization in other rats, the intrauterine desensitization sites were transplanted with hOPCs-1, hOPC-2 and hNSCs-1. At 10 weeks after desensitization with hOPCs-1, immunofluorescence staining using Stem121 revealed that it was positive in the near the corpus callosum of the brain and cerebral cortex in all desensitized groups (Figure 2C), and in desensitized muscles in the i.p.m and i.p.mb groups (Figure 2B). However, immunofluorescence staining of Stem121 was negative in the brain near the corpus callosum and cerebral cortex in the control group (Figure 2C), and in the un-desensitized muscles in the i.p., i.p.m, i.p.b, and i.p.mb groups (Figure 2B). In addition, immunofluorescence staining of Stem121 was positive in the brains that were transplated with hNSCs-1 while negative with hOPCs-2 in the i.p. and i.p.b groups (Figures S1A and S1B). We performed immunofluorescence staining using MBP and Stem121 in all desensitized groups (Figure 2D), and the results revealed that hOPCs could survive and differentiate in the brain.

Survival and inflammatory response of grafts in the brain and muscles of 10-week-old wistar rats

In groups with the transplantation of hOPCs-1, HNA grafts in the brain and muscles of 10-week-old Wistar rats were immunohistochemically stained which revealed that HNA was positive in all desensitized groups while negative in the control group (Figures 3A and S2A). Meanwhile, HNA was positive in i.p. and i.p.b groups with the transplantation of hNSCs-1 while negative in i.p. and i.p.b groups with the transplantation of hOPCs-2 (Figure S2A). The survival of grafts of hOPCs-1 analyzed using the Image-Pro10 software in the rat brain was 75.1%, 75.2%, 55.9%, and 53.4% in the i.p.b, i.p.mb, i.p., and i.p.m groups, respectively (Table 2). In groups with hOPCs-1, brains and muscles were also immunohistochemically stained for CD4 and OX42. The corpus callosum was positive for CD4 and OX42 in the control group, whereas there were few $CD4^+$ T and $OX42^+$ cells in all desensitization groups (Figures 3B and S2B, S2C). In groups with

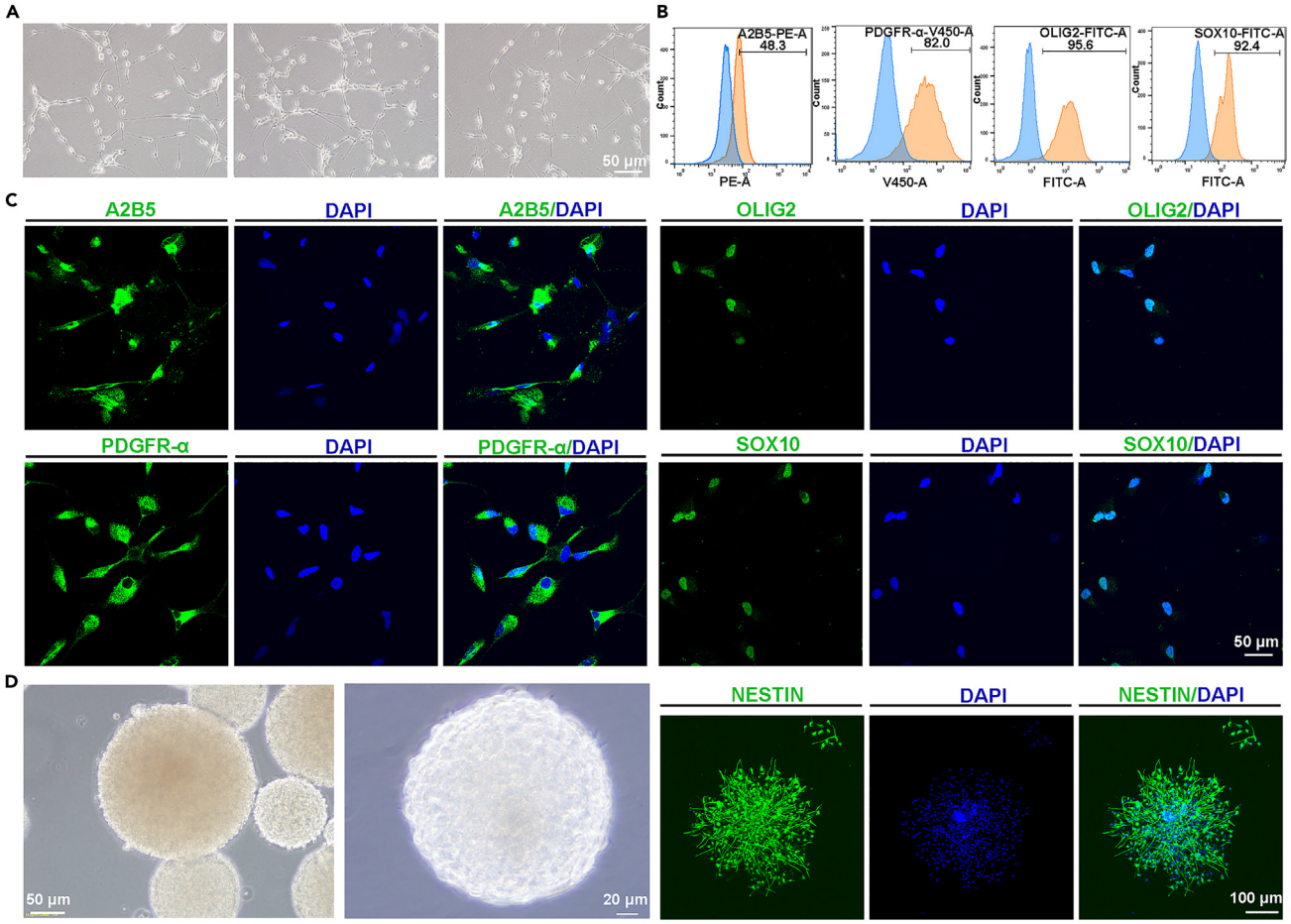

Figure 1. Characterization of human oligodendrocyte precursor cells and neural stem cells

(A) The morphology of hOPCs observed using a phase-contrast microscope. Scale bar, 50 μm.

(B) Proportion of PDGFR-α^+, A2B5$^+$ OLIG2$^+$, and SOX10$^+$ hOPCs was analyzed by flow cytometry.

(C) Immunofluorescence staining of A2B5, PDGFR-α, OLIG2, and SOX10 in hOPCs was confirmed. Scale bar, 50 μm.

(D) The morphology of hNSCs cultured as a suspended state of "neuro-spheres" observed using a phase-contrast microscope. Scale bar, 50 μm and 20 μm; Immunofluorescence staining of NESTIN in hNSCs was confirmed, Scale bar, 50 μm.

hNSCs-1 and hOPCs-2, the corpus callosum was positive for CD4 and OX42 in the i.p. and i.p.b group with the transplantation of hOPCs-2, whereas there were few positive cells i.p. and i.p.b group with hNSCs-1 (Figures S2B and S2C). The un-desensitized muscle group was positive for CD4, whereas the desensitization group had few CD4$^+$ T cells (Figure 3C).

Flow cytometric analysis of peripheral blood mononuclear cells (PMBCs) in peripheral blood of 6 and 10-week-old rats

Flow cytometric analysis of Treg, CD4CD28, CD8CD28, and CD45RC (the detailed antibodies information provided in STAR Methods) in the peripheral blood of six- and 10-week-old rats was performed (Figures 4A and 4B). Treg, a type of helper T cell, can suppress immune rejection when increased. CD4CD28 and CD8CD28 act as the secondary signals for activating CD4 and CD8 helper T cells, respectively; when they decrease, T cell activation also decreases, promoting the development of immune tolerance. The increase in CD45RC, a surface marker of human naive B cells, represents an increase in naive B cells in rats, which also promotes the development of immune tolerance.

In groups with the transplantation of hOPCs-1, flow cytometric analysis (Table 3) revealed that in six-week-old rats (before transplantation), Treg increased in the i.p., i.p.b, and i.p.mb groups compared to that in the

Table 1. Graft survival in the different desensitization protocols

group	Intrauterine desensitization site	Age for desensitization	transplantation site in 6 weeks-old rats	Survival of grafts in Brain[a] (% of cells grafted)
Ctrl	no desensitization	GA15-17days	brain	1.47%
i.p.	i.p.	GA15-17days	brain	55.9%
i.p.m	i.p., muscles	GA15-17days	Brain, Des/no-Des muscle	53.4%
i.p.b	i.p., brain	GA15-17days	Brain, no-Des muscle	75.1%
i.p.mb	i.p., muscles, brain	GA15-17days	Brain, Des/no-Des muscle	75.2%

GA for gestation age. Ctrl/i.p./i.p.m/i.p.b/i.p.mb respectively for group control, i.p., i.p.+muscle, i.p.+brain and i.p.+muscle+brain.
[a]Survival of grafts of brain in 10 weeks-old rats.

control group. CD4CD28 decreased in each intrauterine desensitization group compared to that in the control group, and the CD8CD28 in the i.p. and i.p.mb groups decreased compared to that in the control group (Figure 4C).

In 10-week-old rats (after four weeks of transplantation) with the transplantation of hOPCs-1, Treg increased in the i.p., i.p.b, and i.p.mb groups compared to that in the control group (Figure 4D); In groups with the transplantation of hOPCs-2, Treg did not increased in the i.p., i.p.b, and i.p.mb groups compared to that in the control group (Figure S3A). CD4CD28 and CD8CD28 decreased in each intrauterine desensitization group compared to that in the control group with hOPCs-1 (Figure 4D); In groups with hOPCs-2, CD4CD28 and CD8CD28 did not decrease in the i.p., i.p.b and i.p.mb groups compared to that in the control group (Figure S3A). CD45RC increased in each intrauterine desensitization group compared to that in the control group with hOPCs-1 (Figure 4D); while in group with hOPCs-2, CD45RC decreased in the i.p., and i.p.b groups compared to that in the control group (Figure S3A). The results showed that the desensitization of the same series of cells (hOPCs-1) did not cause activation of T and B cells which was contrary to the Ctrl group, and Treg cells increased. On the contrary, the un-desensitized cells (hOPCs-2) caused activation of T and B cells which was similar to the Ctrl group. CD8CD28 decreased in 10-week-old rats compared to that in 6-week-old rats in i.p., i.p.m, and i.p.b groups(Figure 4E); CD4CD28 decreased in 10-week-old rats compared to that in 6-week-old rats in i.p., and i.p.b groups (Figure S3B); Treg increased in 10-week-old rats compared to that in 6-week-old rats in i.p.m and i.p.b groups (Figures 4E and S3B) which revealed that transplantation of the antigen resulted in an increase in Treg cells and a decrease in activated T cells.

Survival of grafts in the brain of 34-week-old wistar rats

We traced the grafts (hOPCs-1) in the rat brain 34 weeks after intrauterine desensitization using immunofluorescence staining of Stem121 (Figure 5A) and immunohistochemical staining of HNA (Figures 5B and 6A), which revealed that Stem121 and HNA remained positive in the desensitization and cyclosporine (CSA)-treated groups, but negative in the control group (Figures 5A and 5B). In addition, whole brain sections were scanned via 3D-HISTECH and analzed for HNA^+ grafts via Imaris software. The results revealed that the i.p.mb group (brain, n = 3) had the highest number of surviving grafts, followed by the i.p.b group (brain, n = 4), which was equivalent to the CSA-treated group (brain, n = 3), the i.p. (brain, n = 3), and i.p.m (brain, n = 3) groups ranked third and fourth, respectively. The control group (brain, n = 3) had the fewest grafts, indicating that the graft was almost completely rejected (Figure 5C).

To quantify the differentiation capacity of hOPCs-1 into MBP^+ oligodendrocytes, the proportion of $Stem121^+$ cells that were also MBP^+ was determined in i.p., i.p.m, i.p.b, and i.p.mb group (Figure 6B). Images were taken from 20× objective fields per animal, namely, at most three sampling regions per animal. The area fraction of $stem121^+/MBP^+$ was measured using ImageJ. The majority of $Stem121^+$ cells co-expressed MBP, and the area fraction of $stem121^+$ MBP+/$stem121^+$ was 54.42 ± 1.66%, 43.47 ± 6.35%, 80.12 ± 9.81%, and 73.71 ± 10.64% in i.p., i.p.m, i.p.b, and i.p.mb group, respectively (Figure 6C). The differentiation rate of i.p.b group were higher than that of i.p. and i.p.m group, and the differentiation rate of i.p.mb group were higher than that of i.p.m group (Figure 6C).

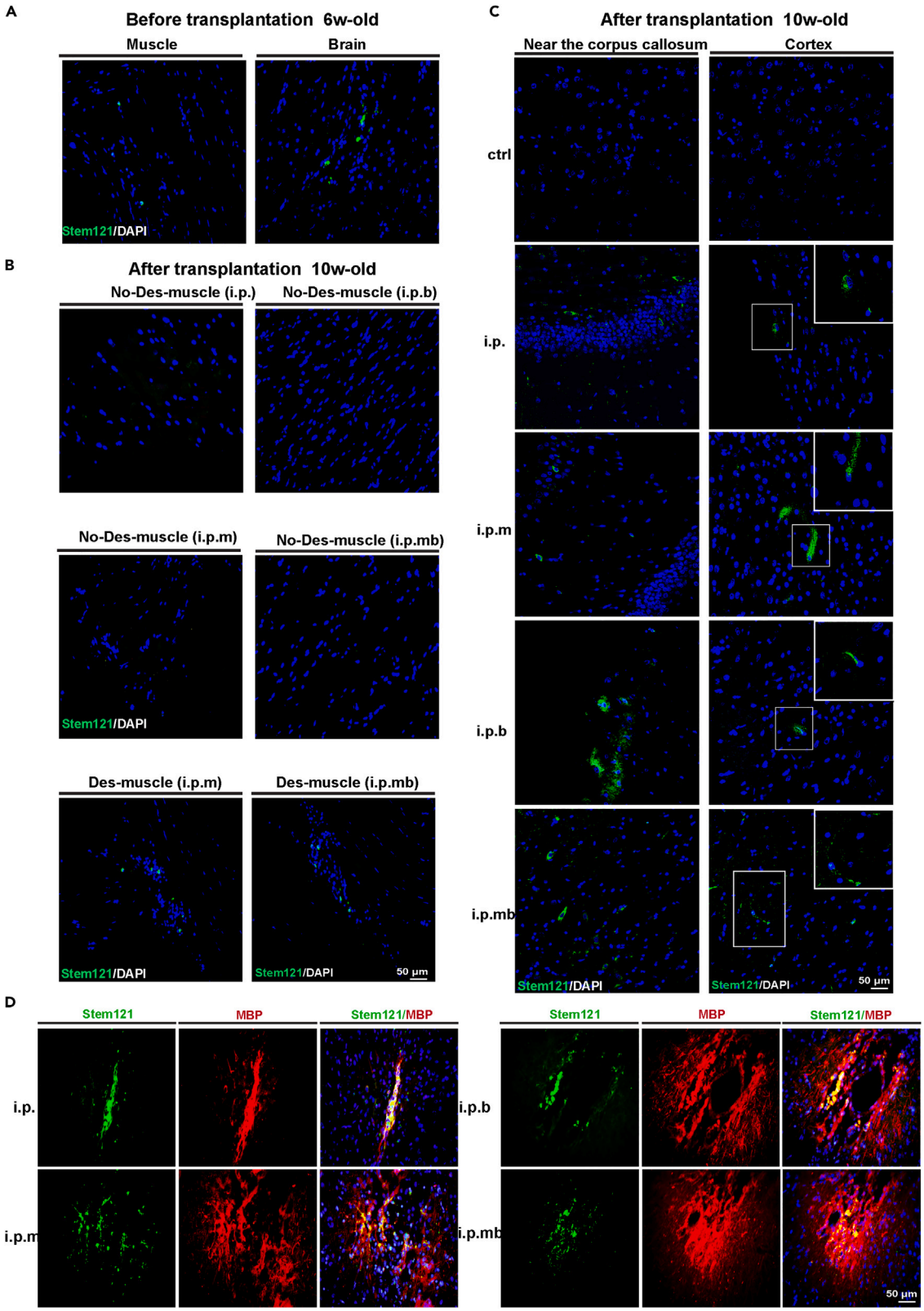
A
Before transplantation 6w-old
Muscle
Brain
Stem121/DAPI
B
After transplantation 10w-old
No-Des-muscle (i.p.)
No-Des-muscle (i.p.b)
No-Des-muscle (i.p.m)
No-Des-muscle (i.p.mb)
Stem121/DAPI
Des-muscle (i.p.m)
Des-muscle (i.p.mb)
Stem121/DAPI
Stem121/DAPI
50 μm
C
After transplantation 10w-old
Near the corpus callosum
Cortex
ctrl
i.p.
i.p.m
i.p.b
i.p.mb
Stem121/DAPI
Stem121/DAPI
50 μm
D
Stem121
MBP
Stem121/MBP
i.p.
i.p.m
Stem121
MBP
Stem121/MBP
i.p.b
i.p.mb
50 μm

Figure 2. Immunofluorescence staining of grafts in 6- and 10-week-old rats in ctrl, i.p., i.p.m, i.p.b, and i.p.mb group with transplantation of hOPCs-1

(A) Immunofluorescence staining of desensitized muscle and brain in six-week-old rats (six weeks after desensitization).

(B) Immunofluorescence staining of desensitized muscles (the left forelimbs in i.p.m and i.p.mb groups) and un-desensitized muscles (the right hind limbs in i.p., i.p.m, i.p.b, and i.p.mb groups) in 10-week-old rats (four weeks after transplantation).

(C) Immunofluorescence staining of the corpus callosum and cerebral cortex in each group in 10-week-old rats (four weeks after transplantation).

(D) Immunofluorescence staining of MBP and Stem121 in desensitization groups. Scale bar, 50 μm i.p., i.p.m, i.p.b, and i.p.mb stands for i.p. (intraperitoneal), i.p.+muscle, i.p.+brain, and i.p.+muscle+brain, respectively.

Inflammatory response of grafts in the brain of 34-week-old wistar rats with hOPCs-1

Immunohistochemical staining of CD4, CD8, and OX42 performed in the corpus callosum in all groups revealed that the control group was positive (Figures 7A–7C). In contrast, the inflammatory reactions of the other desensitization groups and the CSA-treated groups were mild (Figures 7A–7C). We used the Image-Pro 10 software to analyze the cumulative optical density (OD) and area of CD4, CD8, and OX42 to calculate the average OD. The results revealed that the average OD of each desensitization group (slide, n = 8) and CSA-treated group (slide, n = 9) decreased compared to that of the control group (slide, n = 8) (Figure 7D). It is interesting here weather transplanted cells caused increased macrophages in corpus callosum. We performed double-immunofluorescence labeling of grafts with Stem121 and OX42 in 34-week-old rats with hOPCs-1 in Ctrl, i.p., i.p.m i.p.b, and i.p.mb group, respectively. Although the grafts in the Ctrl group were almost completely rejected, there were still $OX42^{+}$ cells in the corpus callosum (Figure S4A). In the intrauterine desensitized abdominal cavity and muscle groups, i.e. i.p. group and i.p.+muscle group, although some grafts survived, there were a small number of $OX42^{+}$ cells around the grafts (Figures S4B and S4C). The brain groups that had undergone intrauterine desensitization, i.e. i.p.+brain and i.p.+-mouse+brain groups, not only survived the grafts, but also had few $OX42^{+}$ cells in the corpus callosum (Figures S4D and S4E).

Mixed lymphocyte culture in 34-week-old wistar rats

We isolated peripheral blood mononuclear cells (PBMCs) from the spleen of 34-week-old rats and co-cultured them with the hOPCs-1, hOPCs-2 and hNSC-1 to establish a mixed lymphocyte culture to study the effects of the grafts on immune cells of recipient rats. We also demonstrated the morphology and growth of cells in the OPC-1+ConA+PBMC, ConA+PBMC, OPC-1+PBMC, and PBMC groups cultured for three and five days (Figure S5A). On the third and fifth days, ConA+PBMCs had clonal spheres with plump and large nuclei. However, in OPC+ConA+PBMC group, the hOPCs inhibited the proliferation of PBMCs (Figure S5A). On the third and fifth days of culture, the number of cells decreased, and the nuclei were smaller in the OPC-1+PBMC and PBMC group without concanavalin A (ConA) stimulation (Figure S5A).

In OPC-1/NSC-1/OPC-2+PBMC group, we collected PBMCs on day five of culture for flow cytometric analysis (Figures 8A and 8B). The results revealed that Treg increased in i.p._OPC-1, i.p.b_OPC-1, i.p._NSC-1, and i.p.b_NSC-1 groups compared to that in the control group ($p < 0.01$) while decreased in the i.p._OPC-2 groups compared to that in the control group ($p < 0.01$). CD4CD28 and CD8CD28 decreased in i.p._OPC-1, i.p.b_OPC-1, i.p._NSC-1, and i.p.b_NSC-1 groups compared to that in the control group (**$p < 0.01$, *$p < 0.05$). CD45RC increased in i.p._OPC-1, i.p.b_OPC-1, and i.p._NSC-1 groups compared to that in the control group (Figure 8C). In OPC-1/NSC-1/OPC-2+ConA+PBMC group, we got similar results showed OPC-1 and NSC-1 reduced the number of activated T/B cells and increased the number of Treg cells compared to that in the control group. However, OPC-2 increased the number of activated T/B cells and reduced or unchanged Treg compared to that in the control group which revealed that T/B cells developed immune tolerance to OPC-1 and NSC-1 (Figure 8D).

In groups with the transplantation of hOPCs-1, Treg increased in the i.p., i.p.b, and i.p.mb groups compared to that in the control group. In all desensitization groups, CD4CD28 decreased compared to that in the control group, and CD45RC increased in the i.p.m and i.p.mb groups compared to that in the control group (Figure S5B). In addition, we used the modfit software to analyze the proliferation of PBMC in each group. The results revealed that the proliferation index of Treg was higher in all desensitization groups than in the control group (Figure S5C). In contrast, the proliferation indexes of CD4CD28 and CD8CD28 were lower in all desensitization groups than in the control group (Figure S5C). Compared to the control group (rats, $n \geq 3$), the proliferation index of CD45RC in the i.p.b and i.p.mb groups increased (Figure S5C).

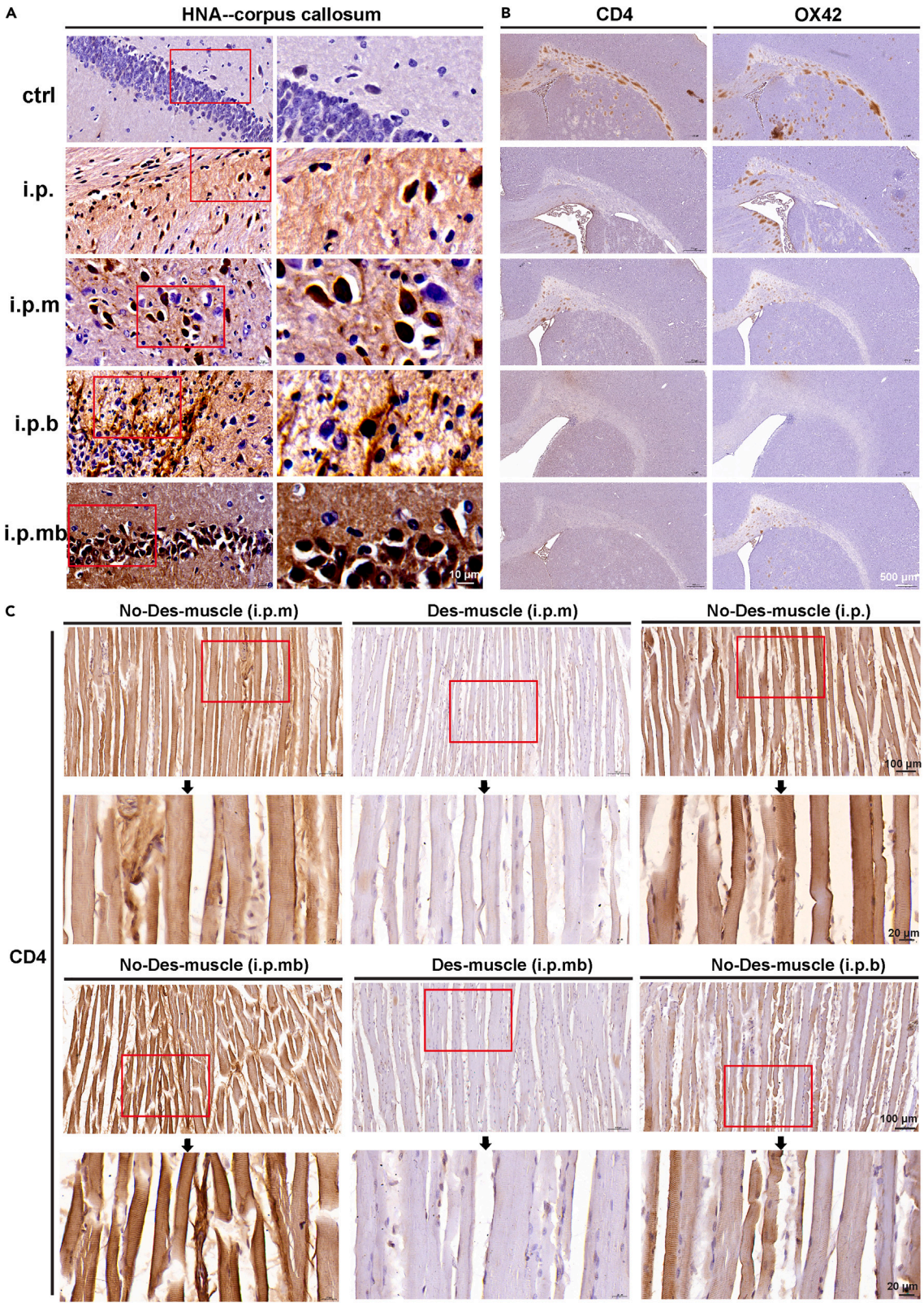
A
HNA--corpus callosum
ctrl
i.p.
i.p.m
i.p.b
i.p.mb
10 μm
B
CD4
OX42
500 μm
C
No-Des-muscle (i.p.m)
Des-muscle (i.p.m)
No-Des-muscle (i.p.)
100 μm
20 μm
CD4
No-Des-muscle (i.p.mb)
Des-muscle (i.p.mb)
No-Des-muscle (i.p.b)
100 μm
20 μm

Figure 3. Immunohistochemical staining of grafts in 10-week-old rats in ctrl, i.p., i.p.m, i.p.b, and i.p.mb group with transplantation of hOPCs-1

(A) Immunohistochemical staining of human nuclear antigen (HNA) in the brain of rats in each group. Scale bar, 20 μm, 10 μm (red box).

(B) Immunohistochemical staining of CD4 and OX42 in the corpus callosum in each group. Scale bar, 500 μm.

(C) Immunohistochemical staining of CD4 in desensitized muscles (the left forelimbs in i.p.m and i.p.mb groups) and un-desensitized muscles (the right hind limbs in i.p., i.p.m, i.p.b, and i.p.mb groups). Scale bar, 100 μm, 20 μm (red box). i.p., i.p.m, i.p.b, and i.p.mb stand for intraperitoneal, i.p.+muscle, i.p.+brain, and i.p.+muscle+brain, respectively.

DISCUSSION

According to the World Health Organization, approximately 15 million premature infants are born every year, and white matter damage is one of the leading causes of death in infants younger than five years.[1,19] Mature OLs differentiated from hOPCs are myelinating cells in the central nervous system.[20,21] Endogenous hOPCs may promote re-myelination in acute demyelinating lesions, but not myelination in chronic demyelinating lesions.[3,22] Transplantation of exogenous hOPCs can effectively promote myelin repair.[6] Immune rejection of exogenous hOPCs transplantation can be reduced using immunosuppressants that are not viable for premature infants, while the immune tolerance induced by desensitization is more beneficial than immunosuppressants for premature infants because of underdeveloped immune system.[13] Nato et al. promote survival and differentiation of Neural precursor cells (NPC) of xenogeneic origin after *in utero* injection of NPC together with adult tolerance inducing tissue extracts.[23] Immune-tolerance of xenografted NPCs needs a double transplant of cells which contains the initial xenografts to desensitization performed usually intraperitoneally before complete development of the host immune system in rat neonates and the second xenografts derived from the same species of the initial one.[24,25]

Desensitization of human cells transplanted into neonatal mice can reduce immune rejection of allografts and induce immune tolerance to allografts in adults. For example, Claire M Kelly et al.[24] injected 1×10^5 human or rat fetal brain-derived neural progenitor cells into the abdominal cavity in newborn and 10-day-old SD rats to induce desensitization. The right lateral striae of the rats were transplanted with $2.5/5\times10^5$ cells of the same type 10–12 weeks later. At 12–40 weeks after transplantation, the grafts injected intraperitoneally at birth remained viable for a long time, while the grafts injected intraperitoneally 10 days after birth were completely rejected which was published *NATURE METHODS*. Shufang Zhang et al.[26] injected 1×10^5 human embryonic stem cells-mesenchymal stem cells (hESC-MSCs) intraperitoneally in neonatal SD rats and then transplanted 2×10^5 hESC-MSCs into the cartilage defect model at six weeks. The results revealed that pre-desensitization of hESC-MSCs was beneficial for joint regeneration. Andreas Heuer et al.[27] injected 1×10^5 hESCs intraperitoneally in neonatal SD rats, and transplanted 2×10^5 hESCs into the striatum at six weeks. This study also revealed that the grafts could survive for a long period of time. Previous studies have suggested that desensitization of human-derived cells in neonatal rats followed by transplantation can prolong the survival of human-derived transplanted cells.

However, this approach that contains the initial xenografts before complete immune development of the host and the second xenografts derived from the same species of the initial one did not always result in long-term xenograft survival which depends on the species of donor, the origin of the cells,[3,6,7] and the strain of the host.[21] There are reports of failure to induce immune tolerance after desensitization. Miroslaw Janowski et al.[28] injected 1×10^5 human glial-restricted precursors (hGRPs) and the neural stem cell line derived from

Table 2. The scheme of flow cytometric analysis

Flow tube	Antibody with fluorescein
Panel1	CD45 PerCP-Cy5.5, CD3-PE, CD4-APC/cy7, CD8-PE/cy7, CD28-APC, CFSE
Isotype1	CD45 PerCP-Cy5.5, CD3-PE, CD4-APC/cy7, CD8-PE/cy7, APC-Mouse IgG1, CFSE
Panel 2	CD45 PerCP-Cy5.5, CD45RC-PE, CFSE
Isotype2	CD45 PerCP-Cy5.5, PE-Mouse IgG1, CFSE
Panel 3	CD45 PerCP-Cy5.5, CD4-APC/cy7, CD25-PE, Foxp3-AlexaFlour647, CFSE
Isotype3	CD45 PerCP-Cy5.5, CD4-APC/cy7, PE-Mouse IgG1, Alexa Fluor® 647-Mouse IgG1, CFSE

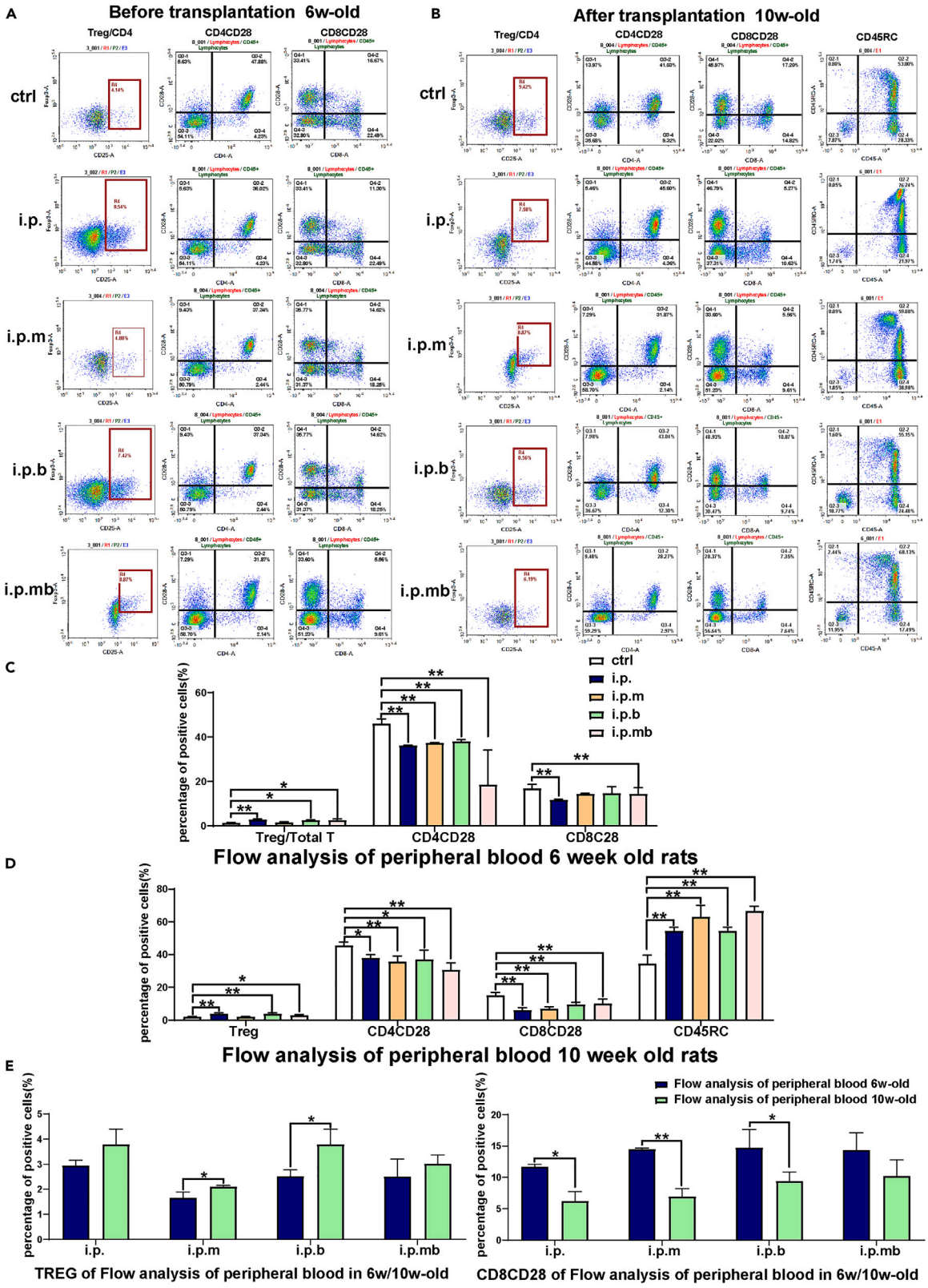
A
Before transplantation 6w-old
Treg/CD4
CD4CD28
CD8CD28
ctrl
i.p.
i.p.m
i.p.b
i.p.mb
B
After transplantation 10w-old
Treg/CD4
CD4CD28
CD8CD28
CD45RC
ctrl
i.p.
i.p.m
i.p.b
i.p.mb
C
percentage of positive cells(%)
Treg/Total T
CD4CD28
CD8C28
ctrl
i.p.
i.p.m
i.p.b
i.p.mb
Flow analysis of peripheral blood 6 week old rats
D
percentage of positive cells(%)
Treg
CD4CD28
CD8CD28
CD45RC
Flow analysis of peripheral blood 10 week old rats
E
percentage of positive cells(%)
i.p.
i.p.m
i.p.b
i.p.mb
TREG of Flow analysis of peripheral blood in 6w/10w-old
Flow analysis of peripheral blood 6w-old
Flow analysis of peripheral blood 10w-old
percentage of positive cells(%)
i.p.
i.p.m
i.p.b
i.p.mb
CD8CD28 of Flow analysis of peripheral blood in 6w/10w-old

Figure 4. Flow cytometric analysis of peripheral blood mononuclear cells (PMBCs) in peripheral blood in 6- and 10-week-old rats in Ctrl, i.p., i.p.m, i.p.b, and i.p.mb group with transplantation of hOPCs-1

(A and B) Flow cytometric analysis of PMBCs in peripheral blood for six- and 10-week-old rats.

(C and D) Histograms of the statistical analysis of flow cytometry of PMBCs for six- and 10-week-old rats, respectively. One-way analysis of variance (ANOVA) test was used. *, $p < 0.05$; **, $p < 0.01$.

(E) Histograms of the statistical analysis of flow cytometry of Treg and CD8CD28 for six- and 10-week-old rats. Independent sample t-test was used for comparison between the experimental group and the control group, *, $p < 0.05$, **, $p < 0.01$. Each group has at least three samples. Data are represented as mean ± SEM.

human umbilical cord blood (HUCB-NSC) into neonatal BALB/c mice and Wistar rats intraperitoneally for desensitization. Six weeks post-transplantation, 3×10^5 hGRP and 2×10^5 HUCB-NSC were transplanted into the brains of the BALB/c mice and Wistar rats, respectively. The bioluminescent imaging signal produced by hGRP gradually decreased in the BALB/c brain and could not be detected 14 days after transplantation. The HNA staining signal of HUCB-NSC cells gradually decreased in the Wistar rat brain and disappeared completely 21 days after transplantation which was published *NATURE METHODS*. Why does allografting into the SD rat induces lifelong immune-tolerance while the very same experiment however, the survival of allografts in Wistar rats and BALB/c mice were gradually decreased and completely rejected?

The development of immune tolerance in neonatal SD rats may be related to their immune development status.[29] At birth, the compartmental structure of the spleen is the periarteriolar aggregation of CD3-positive mononuclear cells, with a slight concentration of CD45RC-positive cells around the periphery of the periarteriolar aggregates. The thymus matures rapidly after postnatal day 14, with a high-density cellular cortex and a lower cellular medulla. Mature T and B cell populations do not appear in the thymus in SD rats until they are nine weeks old. In contrast, Wistar rats have a relatively rapid immune development, with the first T cell precursors reaching the rat thymus anlage on days 13–14 of gestation. On days 15–17 of gestation, $CD4^-CD8^-CD3^-$ triple-negative and $CD45RC^+$ T cells appear. On days 20–21 of gestation, the first mature thymocyte double-positive ($CD4^+CD8^+$) cells appear. The first single positive cells for $CD4^+$ or $CD8^+$ appear in neonatal Wistar rats that have undergone negative and positive selection. One week after birth, $CD4^+CD8^+$ double-positive cell subsets and numerous mature CD4 single-positive cells appear.[30] In BALB/c mice, $CD4^-CD8^-$double negative cells can be observed before 15–17 days of gestation. On days 15–17 of gestation, $CD4^+CD8^+$ double-positive cells appear. BALB/c mice were negatively selected on day 18 of gestation. In neonatal BALB/c mice, few thymus-derived cells already existed in peripheral organs, and immune function had been activated in few cells.[31] The difference in immune development status of the three strains of neonatal mice/rats may be the reason for the success or failure of inducing immune tolerance. Comparing the immune development status of the three experimental models revealed similarities between newborn SD rats, 15–17-day gestational Wistar rats, and 14-day gestational BALB/c mice, which explain why neonatal SD rats can successfully induce immune tolerance while other neonatal strains fail. BALB/c mice at 14 days of gestation were too small and fragile to undergo the intrauterine operation. Therefore, in this study, based on the theory of immature immune development, Wistar rats at 15–17 days of gestation were used to establish an animal model to validate whether immune tolerance can be induced by means of intrauterine desensitization and transplantation.

After desensitization and transplantation, the percentage of lymphocyte subsets and proliferation index were assessed by flow cytometry. Treg cells are crucial in maintaining immune tolerance and repressing antitumor

Table 3. Experimental groups performed according to different desensitization methods and different transplanted cells

group	OPC-1[a]	NSC-1	OPC-2	OPC-1[b]	sum
Ctrl[c]	3	3	3	3	12
i.p.[c]	3	2	3	3	11
i.p.+muscle[c]	2			3	5
i.p.+brain[c]	3	3	3	4	13
i.p.+muscle+brain[c]	4			3	7
CSA[c]				3	3

[a]Wistar rats after 10 weeks of desensitization.

[b]Wistar rats after 34 weeks of desensitization, c the number of the rats in each group.

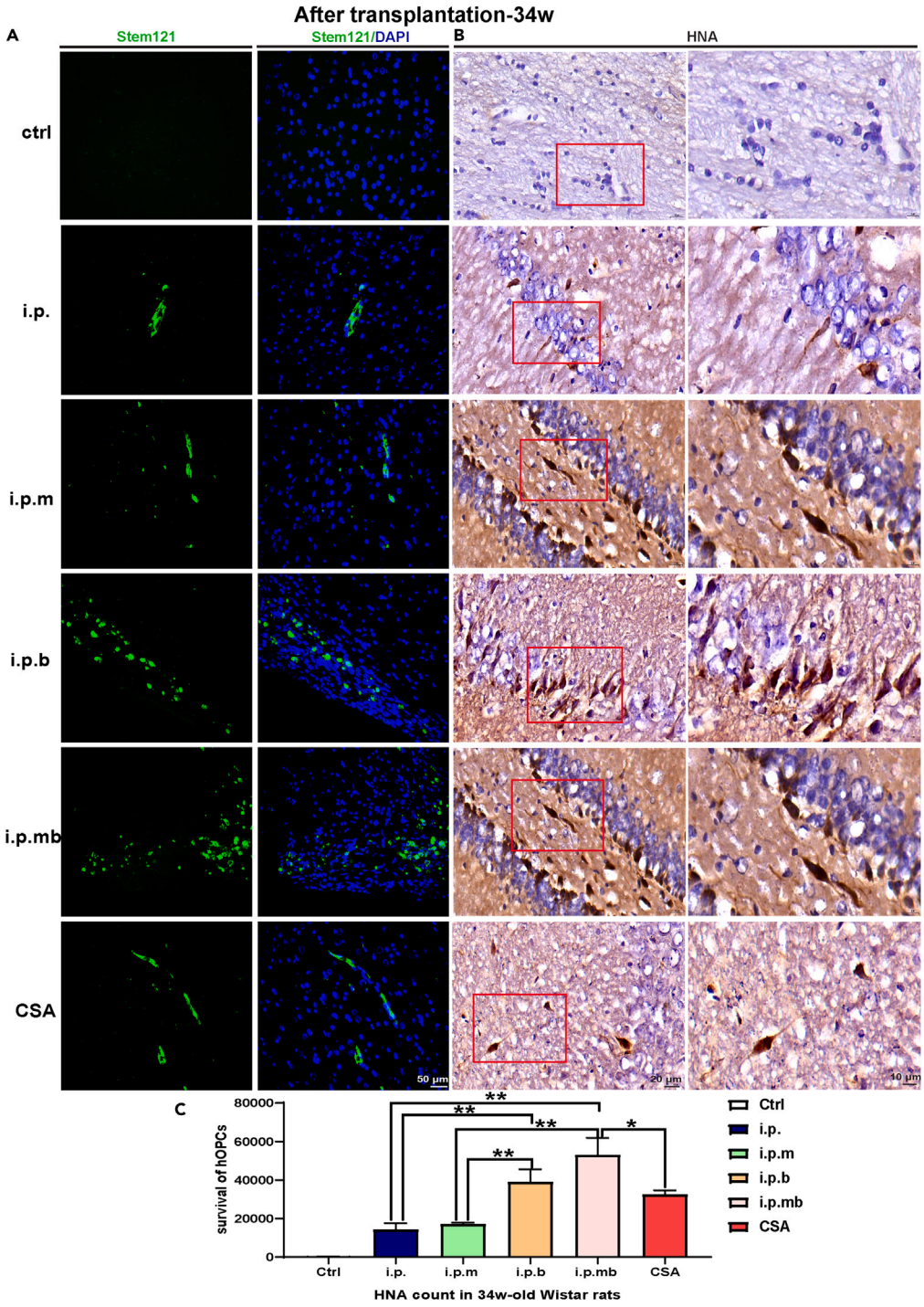

Figure 5. Immunohistochemical and immunofluorescence staining of grafts in 34-week-old rats in ctrl, i.p., i.p.m, i.p.b, and i.p.mb group with transplantation of hOPCs-1

(A) Immunofluorescence staining of Stem121 in the brain of 34-week-old rats. Scale bar, 50 μm.

(B) Immunohistochemical staining of HNA in the brain of 34-week-old rats. Scale bar, 20 μm, 10 μm (red box).

(C) Histograms of the statistical analysis of HNA^+ grafts in 34-week-old Wistar rats. One-way analysis of variance (ANOVA) test was used. *, $p < 0.05$; **, $p < 0.01$. Data are represented as mean ± SEM.

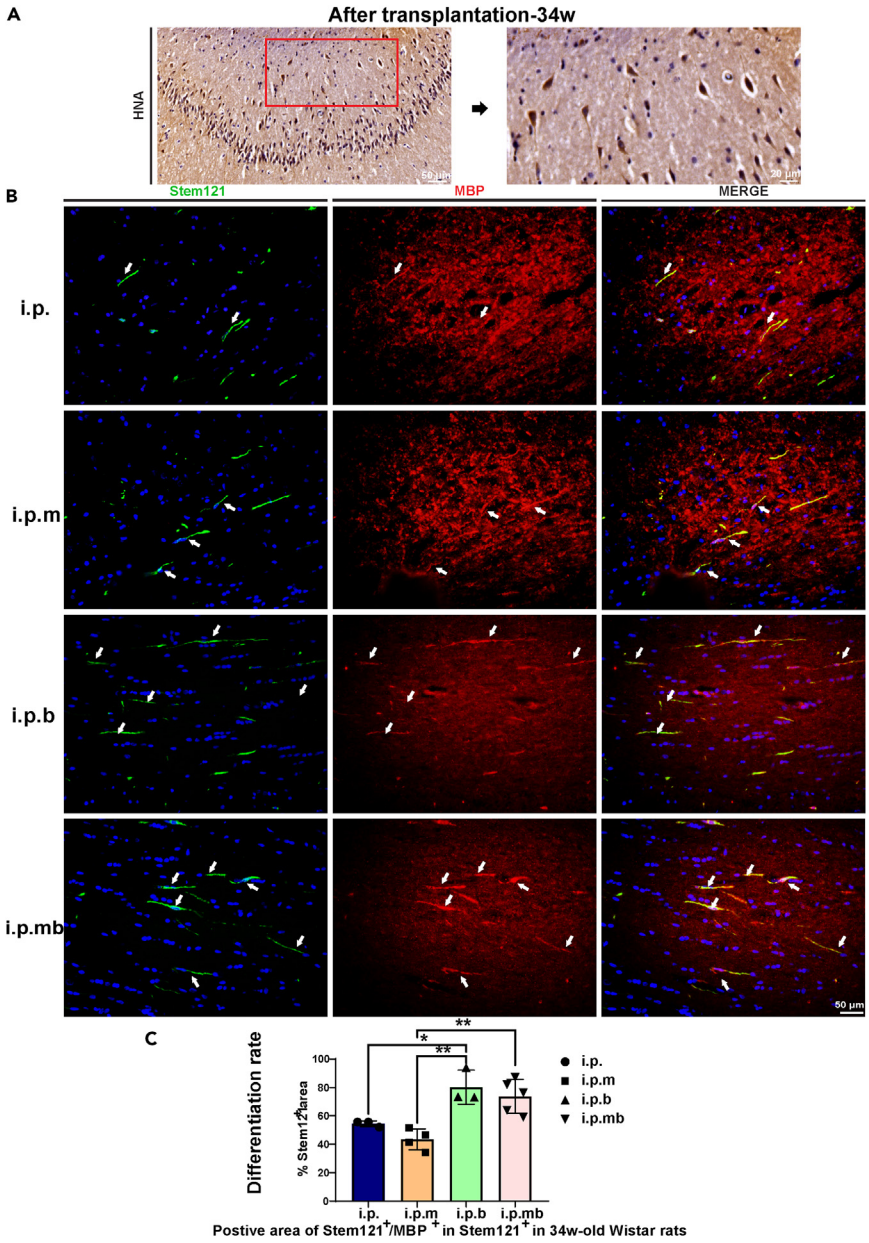

Figure 6. Differentiation rate of grafts in 34-week-old rats in i.p., i.p.m, i.p.b, and i.p.mb group with transplantation of hOPCs-1

(A) Immunohistochemical staining of HNA in the brain of 34-week-old rats in i.p.mb group. Scale bar, 50, 20 (red box) μm.

(B) Immunofluorescence staining of Stem121 and MBP in the brain of 34-week-old rats in i.p., i.p.m, i.p.b, and i.p.mb group. Scale bar, 50 μm.

(C) Histograms of the statistical analysis of Stem121^{+}/MBP^{+} area in Stem121^{+} area in 34-week-old Wistar rats. One-way analysis of variance (ANOVA) test was used. *, $p < 0.05$; **, $p < 0.01$. Data are represented as mean ± SEM.

immunity,[32,33] inhibiting direct and indirect xenogeneic responses of T cells, and suppressing the activation of B cells and macrophages and functioning of antigen-presenting cells.[33] CD4^{+}CD25^{+}FoxP3^{+}T cells suppress inflammation by secreting cytokines, enhancing central and peripheral tolerance, and blunting responses to self and external antigens. Tregs reduce sensitization and resolve inflammation.[12,34] CD28, a transmembrane glycoprotein, is a member of the immunoglobulin superfamily.[35] When CD28 expression is significantly low, the B7/CD28 counter-receptor co-stimulation pathway is disrupted. A decrease in the secondary signal of the activation of CD4 and CD8 T cell (CD4CD28/CD8CD28) results in T cells not being fully activated.

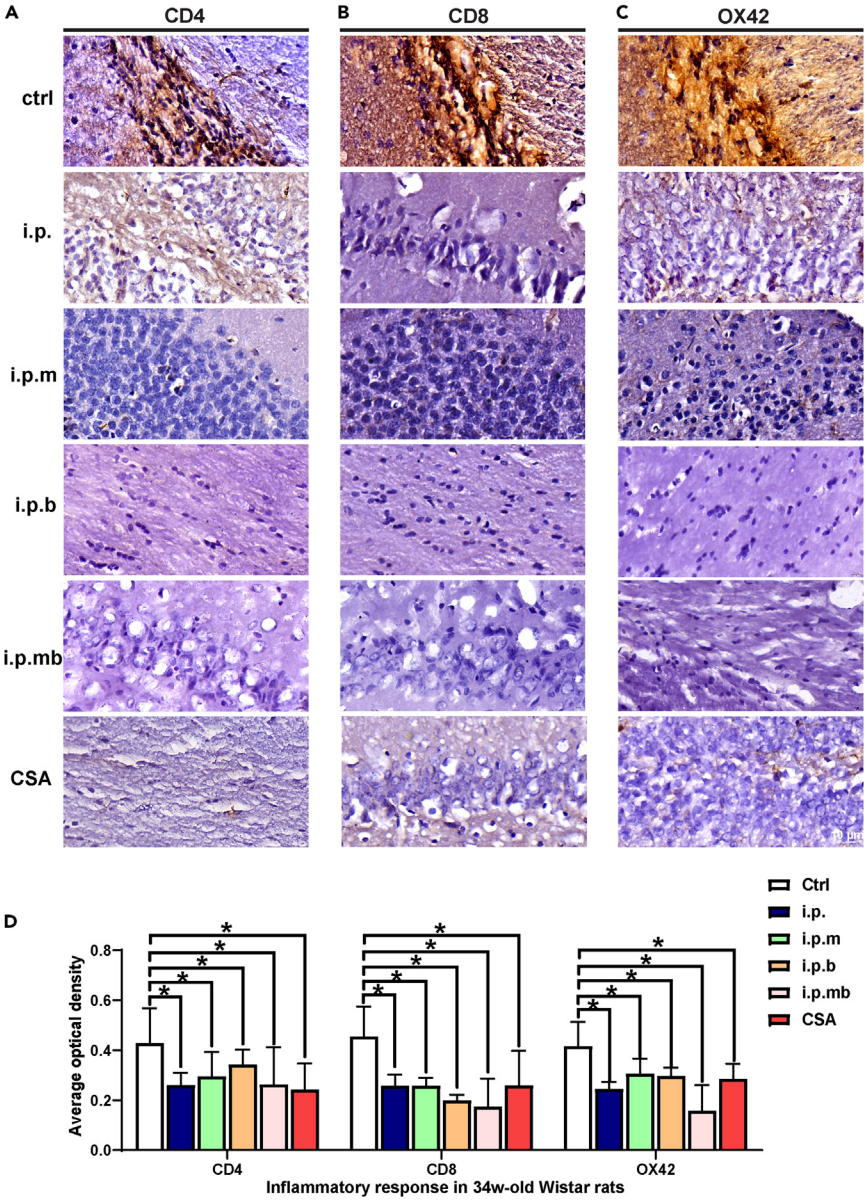

Figure 7. Immunohistochemical staining of CD4, CD8, and OX42 in 34-week-old rats in Ctrl, i.p., i.p.m, i.p.b and i.p.mb group with transplantation of hOPCs-1

(A–C) Immunohistochemical staining of CD4, CD8, and OX42 in 34-week-old rats, Scale bar, 10 μm.

(D) Histograms of the statistical analysis of the average OD of CD4, CD8, and OX42 in 34-week-old Wistar rats. Independent sample t-test was used for comparison between the experimental group and the control group, *, $p < 0.05$. Each group has at least three samples. Data are represented as mean ± SEM.

Lymphocyte function declines when $CD4^+CD28^+$ and $CD8^+CD28^+$ signals are attenuated[12] which will blunt immune rejection. CD45 signaling is necessary for efficient T cell activation. An increase in naive B cells (CD45RC) led to a decrease in immune cloning. CD45RC is a surface marker of naive B cells in rats that induces stable immune tolerance.[36] In this study, flow analysis of peripheral blood and mixed culture of hOPCs and lymphocytes showed that Treg and CD45RC, two key indicators of immune tolerance, were significantly higher in the desensitization groups than those in the control group; in contrast, CD4CD28 and CD8CD28, the key indicators of immune rejection, were significantly lower in the desensitization groups than those in the control group; CD4CD28 and CD8CD28 were significantly lower in 10-week-old rats than those in 6-week-old rats which indicated the recipient reduced the number of activated T cells caused by retransplanted cells. These

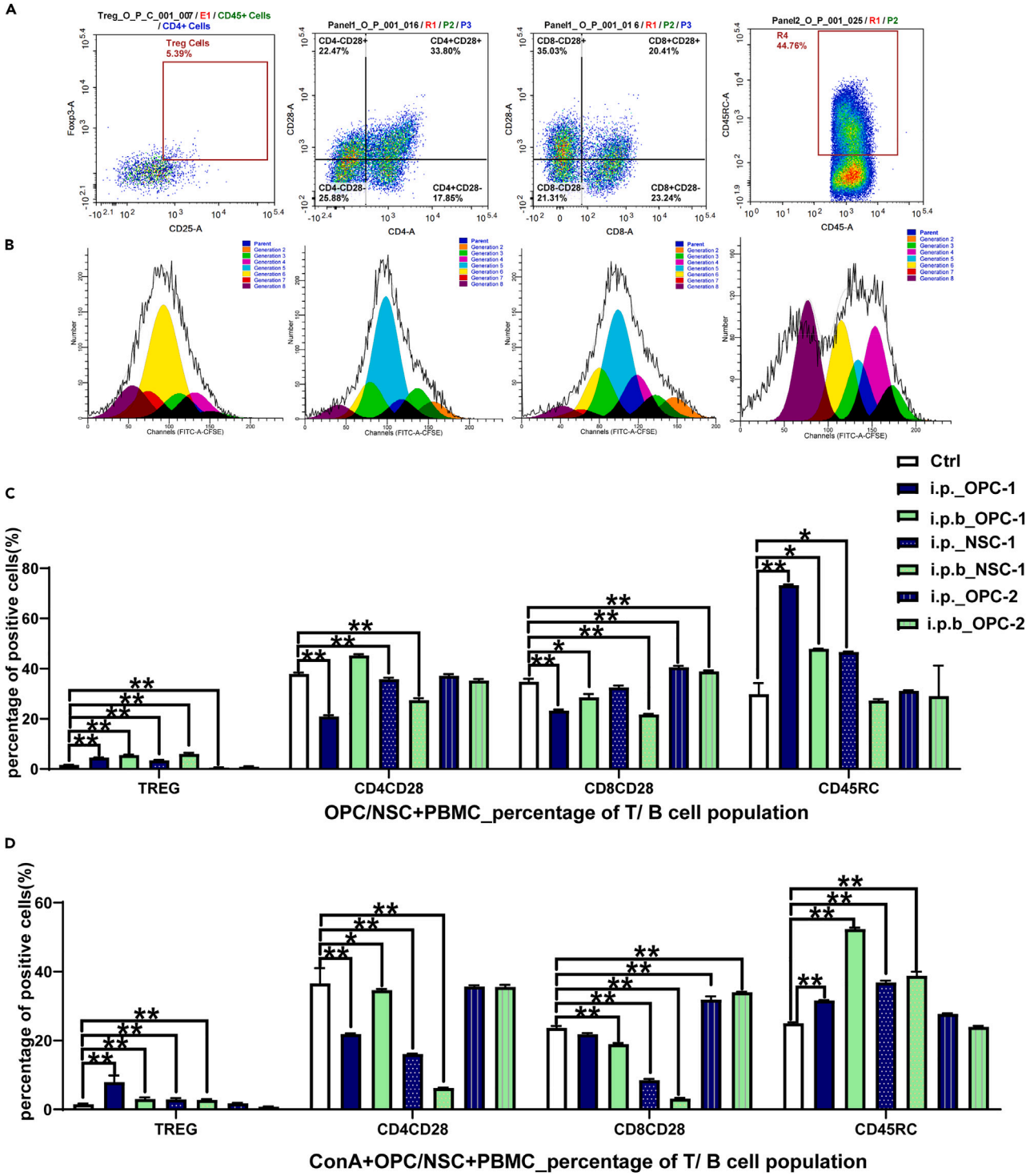

Figure 8. Mixed lymphocyte culture of PBMC of 34-week-old rats in Ctrl, i.p., and i.p.b group with transplantation of hOPCs-1, and i.p., and i.p.b group with transplantation of hNSCs-1 and hOPCs-2

(A and B) Treg, CD4CD28, CD8CD28, and CD45RC of PMBCs in mixed lymphocyte culture for 34-week-old rats.

(C and D) For OPC/NSC+PBMC and ConA+OPC/NSC+PBMC, histograms of the statistical analysis of flow analysis of T/B cells population in mixed lymphocyte culture for 34-week-old rats in Ctrl, i.p._OPC-1, i.p.b_OPC-1, i.p._NSC-1, i.p.b_NSC-1, i.p._OPC-1, and i.p.b_OPC-2 group. Independent sample t-test was used for comparison between the experimental group and the control group, *, $p < 0.05$, **, $p < 0.01$. Each group has at least three samples. Data are represented as mean ± SEM.

results were basically consistent with the increase or decrease of these markers which were beneficial in inducing immune tolerance to the grafts. Moreover, by analyzing the reported studies, and the results of our successful induction of immune tolerance, Treg, CD45RC, CD4CD28, and CD28 can be used as indicators to guide the successful induction of immune tolerance.

Regarding grafts, T cells of the host encounter the allograft through the antigen-presenting cells of the recipient and attack the allografts, resulting in graft rejection. The allogeneic grafts persisted for four weeks after transplantation in desensitized muscles but not in un-desensitized muscles. Based on immunohistochemical staining, the average OD of CD4 in the desensitized muscles was lower than that in the un-desensitized muscles. Both confirm the hypothesis that desensitization induces immune tolerance in peripheral muscles. Moreover, the average OD of CD4, CD8, and OX42 of the brains in intrauterine desensitization group was lower than in the control group. This indicates that intrauterine desensitization also can reduce the inflammatory response caused by the transplantation of cells in the central nervous system.

The central nervous system has been considered an immunologically preferential site for transplantation due to the special structure of the brain; however, grafts in the central nervous system can still be rejected by the immune system, resulting in poor neural graft survival and impaired functional recovery.[37–39] Microglia and macrophages are major immune rejection mediators in the central nervous system.[40] Claire M Kelly et al. confirmed that, after striatal desensitization in neonatal SD rats, the inflammatory response of the striatum was less than that before allogeneic desensitization.[24] Central immune tolerance can be successfully induced after allogeneic desensitization and transplantation.[24] The survival and differentiation of the hOPCs-1 further demonstrated the success of central immune tolerance. Allografts were implanted in the brain and muscles based on intrauterine abdominal desensitization to explore the difference in immune tolerance between the central nervous system and periphery, *in utero*. Nonetheless, the number of surviving allografts in desensitized brains was higher than that in the un-desensitized brain, the allografts in the un-desensitized brain survived from 10 weeks up to 34 weeks. Whlie there were no surviving allografts in the un-desensitized muscles in 10-week-old Wistar rats. This indicates that the central nervous system is relatively tolerant to transplantation and more likely to develop immune tolerance. The comparison of i.p., i.p.m, i.p.b, and i.p.mb desensitization groups showed that the survival of allografts in the i.p.b and i.p.mb desensitization groups with desensitized brains was higher than that in the i.p. and i.p.m desensitization groups with un-desensitized brains. That is, the grafts of the desensitized brain survived were more than those of the un-desensitized brain. This indicates that the survival rate of allogeneic grafts after multiple central transplants has a cumulative effect.

Future research is needed to determine whether the immune tolerance induced by intrauterine desensitization in Wistar rats can be applied to human preterm infants. Therefore, we analyzed whether the immune development of preterm infants is suitable for the induction of immune tolerance through desensitization. At 12 gestation weeks, lymph nodes and Peyer's patches lymphoid tissue appear in the human fetus.[41,42] At 16–20 gestation weeks, T cells migrate to form a peripheral T cell pool, and developing T cells are in close contact with thymic epithelial cells. At 20 gestation weeks, the thymus begins to develop. The development of Tregs peaks at 23–32 gestation weeks. After birth, neutrophils grow exponentially, and the number of neutrophils in the first week of life may even exceed adult levels. The absolute number of natural killer cells peaks at birth and then gradually declines until it reaches adult levels at age five. One week after birth, the number of lymphocytes in newborns increase significantly; therefore, lymphocyte development and maturation are completed mainly after birth. T cell levels increase yearly after birth and then decrease to the adult level in children aged 3 to 7 years old. The spleen remains underdeveloped until the age of two.[43,44] White matter damage in preterm infants is likely to occur between 28 and 32 gestation weeks.[45] Treg development also peaks at this time,[17] and immune tolerance can be easily developed. Desensitization of premature infants is expected to induce immune tolerance and alleviate immune rejection. The results of this study are expected to guide the induction of immune tolerance through desensitization in preterm infants.

In this study, desensitized Wistar rats developed immune tolerance to transplanted hOPCs-1 and hNSCs-1, and rejected hOPCs-2. Additionally, intrauterine desensitization enabled hOPCs-1 survival in the center and periphery, and desensitization reduced the inflammatory response to transplantation. The results included immune tolerance in rats treated by intrauterine desensitization, long-term grafts survival in the host, and reduction of immune rejection caused by grafts. We also found that the central nervous system is in a relatively tolerant to transplantation. Furthermore, Treg, CD45RC, CD4CD28, and CD8CD28 can be used as indicators to guide the successful induction of immune tolerance, and multiple

central transplants have a cumulative effect. In future research, the animal model of immune tolerance induced by intrauterine desensitization in Wistar rats should be combined with the WMI model to observe the myelin repair effect of grafts on WMI. We also should focus on the effect of desensitization and transplantation on graft rejection and disease improvement in premature infants.

Limitations of the study

In the model of intrauterine desensitization, the fetal brain was too small to desensitize accurately near the corpus callosum resulting in that we cannot observe whether desensitized cells can differentiate. We can't tell whether myelination was caused by desensitized cells or transplanted cells. In general, we cannot judge whether the surviving grafts are desensitized cells, transplanted cells, or both.

STAR★METHODS

Detailed methods are provided in the online version of this paper and include the following:

- KEY RESOURCES TABLE
- RESOURCE AVAILABILITY
  - Lead contact
  - Materials availability
  - Data and code availability
- EXPERIMENTAL MODEL AND SUBJECT DETAILS
  - For experimental animal models
  - For cell lines
- METHOD DETAILS
  - Preparation of hNSCs and hOPCs for desensitization and transplantation
  - Intrauterine desensitization
  - Flow cytometric analysis of immune cells in rat peripheral blood
  - Transplantation
  - Immunohistochemical and immunofluorescence staining
  - Mixed lymphocyte culture
- QUANTIFICATION AND STATISTICAL ANALYSIS
  - Quantification of graft cells
  - Statistical analysis

SUPPLEMENTAL INFORMATION

Supplemental information can be found online at https://doi.org/10.1016/j.isci.2023.106647.

ACKNOWLEDGMENTS

This work was supported by the National Key Research and Development Program of China (2017YFA0104200).

AUTHOR CONTRIBUTIONS

Y.D., L.Z., Q.-S.Q., F.-Z.C., and Y.-Y.X. conceived of the presented idea and designed the experiments. Y.D., Q.-S.Q., Y.-Y.X., W.Q., W.P.-L., F.Z., Q.G., J.Z., X.L., X.H.-W., and H.T.-L. performed the experiments. Y.D. and Q.-S.Q. analyzed the experimental data and wrote the manuscript, identified and declared conflicts of interest on behalf of all authors, and archived unprocessed data and ensured that figures accurately present the original data. L.Z., R.Q.-Y., and F.-Z.C. provided technical and material support, supervised the work, are responsible for all data, figures, and text, ensured that authorship is granted appropriately to contributors, ensured adherence to all editorial and submission policies. All authors approve the content and submission of the paper, as well as edits made through the revision and production processes.

DECLARATION OF INTERESTS

The authors declare no competing interests.

INCLUSION AND DIVERSITY

We worked to ensure sex balance in the selection of non-human subjects. We worked to ensure diversity in experimental samples through the selection of the cell lines.

ETHICS APPROVAL AND CONSENT TO PARTICIPATE

This study was approved by the Ethics Committees of Beijing Center for Physical & Chemical Analysis (SWDW-01-03).

Received: October 21, 2022
Revised: March 2, 2023
Accepted: April 5, 2023
Published: April 11, 2023

REFERENCES

1. Mantoo, M.R., Deorari, A.K., Jana, M., Agarwal, R., Sankar, M.J., and Thukral, A. (2021). Preterm white matter injury: a prospective cohort study. Indian Pediatr. *58*, 922–927.

2. Wang, X., Zang, J., Yang, Y., Lu, S., Guan, Q., Ye, D., Wang, Z., Zhou, H., Li, K., Wang, Q., et al. (2021). Transplanted human oligodendrocyte progenitor cells restore neurobehavioral deficits in a rat model of preterm white matter injury. Front. Neurol. *12*, 749244. https://doi.org/10.3389/fneur.2021.749244.

3. Yeung, M.S.Y., Zdunek, S., Bergmann, O., Bernard, S., Salehpour, M., Alkass, K., Perl, S., Tisdale, J., Possnert, G., Brundin, L., et al. (2014). Dynamics of oligodendrocyte generation and myelination in the human brain. Cell *159*, 766–774. https://doi.org/10.1016/j.cell.2014.10.011.

4. Back, S.A. (2017). White matter injury in the preterm infant: pathology and mechanisms. Acta Neuropathol. *134*, 331–349. https://doi.org/10.1007/s00401-017-1718-6.

5. Alizadeh, A., Dyck, S.M., and Karimi-Abdolrezaee, S. (2015). Myelin damage and repair in pathologic CNS: challenges and prospects. Front. Mol. Neurosci. *8*, 35. https://doi.org/10.3389/fnmol.2015.00035.

6. Skaper, S.D. (2019). Oligodendrocyte precursor cells as a therapeutic target for demyelinating diseases. Prog. Brain Res. *245*, 119–144. https://doi.org/10.1016/bs.pbr.2019.03.013.

7. Zhou, H., He, Y., Wang, Z., Wang, Q., Hu, C., Wang, X., Lu, S., Li, K., Yang, Y., and Luan, Z. (2021). Identifying the functions of two biomarkers in human oligodendrocyte progenitor cell development. J. Transl. Med. *19*, 188. https://doi.org/10.1186/s12967-021-02857-8.

8. Piao, J., Major, T., Auyeung, G., Policarpio, E., Menon, J., Droms, L., Gutin, P., Uryu, K., Tchieu, J., Soulet, D., and Tabar, V. (2015). Human embryonic stem cell-derived oligodendrocyte progenitors remyelinate the brain and rescue behavioral deficits following radiation. Cell Stem Cell *16*, 198–210. https://doi.org/10.1016/j.stem.2015.01.004.

9. Zhang, C., Guan, Q., Shi, H., Cao, L., Liu, J., Gao, Z., Zhu, W., Yang, Y., Luan, Z., and Yao, R. (2021). A novel RIP1/RIP3 dual inhibitor promoted OPC survival and myelination in a rat neonatal white matter injury model with hOPC graft. Stem Cell Res. Ther. *12*, 462. https://doi.org/10.1186/s13287-021-02532-1.

10. Kim, T.K., Park, D., Ban, Y.H., Cha, Y., An, E.S., Choi, J., Choi, E.K., and Kim, Y.B. (2018). Improvement by human oligodendrocyte progenitor cells of neurobehavioral disorders in an experimental model of neonatal periventricular leukomalacia. Cell Transplant. *27*, 1168–1177. https://doi.org/10.1177/0963689718781330.

11. Salama, A.D., Womer, K.L., and Sayegh, M.H. (2007). Clinical transplantation tolerance: many rivers to cross. J. Immunol. *178*, 5419–5423. https://doi.org/10.4049/jimmunol.178.9.5419.

12. Sakaguchi, S., Sakaguchi, N., Asano, M., Itoh, M., and Toda, M. (2011). Pillars article: immunologic self-tolerance maintained by activated T cells expressing IL-2 receptor alpha-chains (CD25). Breakdown of a single mechanism of self-tolerance causes various autoimmune diseases. J. Immunol. *186*, 3808–3821.

13. Yang, Y.L., Dou, K.F., and Li, K.Z. (2003). Influence of intrauterine injection of rat fetal hepatocytes on rejection of rat liver transplantation. World J. Gastroenterol. *9*, 137–140. https://doi.org/10.3748/wjg.v9.i1.137.

14. Prévot, A., Martini, S., and Guignard, J.P. (2001). [Exposure in utero to immunosuppressives]. Rev. Med. Suisse Romande *121*, 283–291.

15. Selvanathan, T., Guo, T., Kwan, E., Chau, V., Brant, R., Synnes, A.R., Grunau, R.E., and Miller, S.P. (2022). Head circumference, total cerebral volume and neurodevelopment in preterm neonates. Arch. Dis. Child. Fetal Neonatal Ed. *107*, 181–187. https://doi.org/10.1136/archdischild-2020-321397.

16. Hayward, A.R. (1981). Development of lymphocyte responses and interactions in the human fetus and newborn. Immunol. Rev. *57*, 39–60. https://doi.org/10.1111/j.1600-065x.1981.tb00441.x.

17. Darrigues, J., van Meerwijk, J.P.M., and Romagnoli, P. (2018). Age-Dependent changes in regulatory T lymphocyte development and function: a mini-review. Gerontology *64*, 28–35. https://doi.org/10.1159/000478044.

18. Rackaityte, E., and Halkias, J. (2020). Mechanisms of fetal T cell tolerance and immune regulation. Front. Immunol. *11*, 588. https://doi.org/10.3389/fimmu.2020.00588.

19. Agut, T., Alarcon, A., Cabañas, F., Bartocci, M., Martinez-Biarge, M., and Horsch, S.; eurUS.brain group (2020). Preterm white matter injury: ultrasound diagnosis and classification. Pediatr. Res. *87*, 37–49. https://doi.org/10.1038/s41390-020-0781-1.

20. Motavaf, M., and Piao, X. (2021). Oligodendrocyte development and implication in perinatal white matter injury. Front. Cell. Neurosci. *15*, 764486. https://doi.org/10.3389/fncel.2021.764486.

21. Marangon, D., Caporale, N., Boccazzi, M., Abbracchio, M.P., Testa, G., and Lecca, D. (2021). Novel in vitro experimental approaches to study myelination and remyelination in the central nervous system. Front. Cell. Neurosci. *15*, 748849. https://doi.org/10.3389/fncel.2021.748849.

22. Niu, J., Yu, G., Wang, X., Xia, W., Wang, Y., Hoi, K.K., Mei, F., Xiao, L., Chan, J.R., and Fancy, S.P.J. (2021). Oligodendroglial ring finger protein Rnf43 is an essential injury-specific regulator of oligodendrocyte maturation. Neuron *109*, 3104–3118.e6. https://doi.org/10.1016/j.neuron.2021.07.018.

23. Nato, G., Corti, A., Parmigiani, E., Jachetti, E., Lecis, D., Colombo, M.P., Delia, D., Buffo, A., and Magrassi, L. (2021). Immune-tolerance to human iPS-derived neural progenitors xenografted into the immature cerebellum is overridden by species-specific differences in differentiation timing. Sci. Rep. *11*, 651. https://doi.org/10.1038/s41598-020-79502-9.

24. Kelly, C.M., Precious, S.V., Scherf, C., Penketh, R., Amso, N.N., Battersby, A., Allen, N.D., Dunnett, S.B., and Rosser, A.E. (2009). Neonatal desensitization allows long-term survival of neural xenotransplants without immunosuppression. Nat. Methods *6*,

271–273. https://doi.org/10.1038/nmeth.1308.

25. Magrassi, L., Nato, G., Delia, D., and Buffo, A. (2022). Cell-autonomous processes that impair xenograft survival into the cerebellum. Cerebellum *21*, 821–825. https://doi.org/10.1007/s12311-022-01414-3.

26. Zhang, S., Jiang, Y.Z., Zhang, W., Chen, L., Tong, T., Liu, W., Mu, Q., Liu, H., Ji, J., Ouyang, H.W., and Zou, X. (2013). Neonatal desensitization supports long-term survival and functional integration of human embryonic stem cell-derived mesenchymal stem cells in rat joint cartilage without immunosuppression. Stem Cell. Dev. *22*, 90–101. https://doi.org/10.1089/scd.2012.0116.

27. Heuer, A., Kirkeby, A., Pfisterer, U., Jönsson, M.E., and Parmar, M. (2016). hESC-derived neural progenitors prevent xenograft rejection through neonatal desensitisation. Exp. Neurol. *282*, 78–85. https://doi.org/10.1016/j.expneurol.2016.05.027.

28. Janowski, M., Jablonska, A., Kozlowska, H., Orukari, I., Bernard, S., Bulte, J.W.M., Lukomska, B., and Walczak, P. (2012). Neonatal desensitization does not universally prevent xenograft rejection. Nat. Methods *9*, 856–858. author reply 858. https://doi.org/10.1038/nmeth.2146.

29. Parker, G.A., Picut, C.A., Swanson, C., and Toot, J.D. (2015). Histologic features of postnatal development of immune system organs in the sprague-dawley rat. Toxicol. Pathol. *43*, 794–815. https://doi.org/10.1177/0192623315578720.

30. Vicente, A., Varas, A., Acedón, R.S., Jiménez, E., Muñoz, J.J., and Zapata, A.G. (1998). Appearance and maturation of T-cell subsets during rat thymus ontogeny. Dev. Immunol. *5*, 319–331. https://doi.org/10.1155/1998/24239.

31. Xiao, S.Y., Li, Y., and Chen, W.F. (2003). Kinetics of thymocyte developmental process in fetal and neonatal mice. Cell Res. *13*, 265–273. https://doi.org/10.1038/sj.cr.7290171.

32. Duggleby, R., Danby, R.D., Madrigal, J.A., and Saudemont, A. (2018). Clinical grade regulatory CD4(+) T cells (Tregs): moving toward cellular-based immunomodulatory therapies. Front. Immunol. *9*, 252. https://doi.org/10.3389/fimmu.2018.00252.

33. Xu, C., Sun, S., Johnson, T., Qi, R., Zhang, S., Zhang, J., and Yang, K. (2021). The glutathione peroxidase Gpx4 prevents lipid peroxidation and ferroptosis to sustain Treg cell activation and suppression of antitumor immunity. Cell Rep. *35*, 109235. https://doi.org/10.1016/j.celrep.2021.109235.

34. Balmert, S.C., Donahue, C., Vu, J.R., Erdos, G., Falo, L.D., Jr., and Little, S.R. (2017). In vivo induction of regulatory T cells promotes allergen tolerance and suppresses allergic contact dermatitis. J. Contr. Release *261*, 223–233. https://doi.org/10.1016/j.jconrel.2017.07.006.

35. Asai, T., Choi, B.K., Kwon, P.M., Kim, W.Y., Kim, J.D., Vinay, D.S., Gebhardt, B.M., and Kwon, B.S. (2007). Blockade of the 4-1BB (CD137)/4-1BBL and/or CD28/CD80/CD86 costimulatory pathways promotes corneal allograft survival in mice. Immunology *121*, 349–358. https://doi.org/10.1111/j.1365-2567.2007.02581.x.

36. Mirzakhani, M., Shahbazi, M., Oliaei, F., and Mohammadnia-Afrouzi, M. (2019). Immunological biomarkers of tolerance in human kidney transplantation: an updated literature review. J. Cell. Physiol. *234*, 5762–5774. https://doi.org/10.1002/jcp.27480.

37. Vadori, M., and Cozzi, E. (2015). The immunological barriers to xenotransplantation. Tissue Antigens *86*, 239–253. https://doi.org/10.1111/tan.12669.

38. Tanemura, M., Yin, D., Chong, A.S., and Galili, U. (2000). Differential immune responses to alpha-gal epitopes on xenografts and allografts: implications for accommodation in xenotransplantation. J. Clin. Invest. *105*, 301–310. https://doi.org/10.1172/JCI7358.

39. Arad, T., Fainstein, N., Goldfarb, S., Lachish, M., Ganz, T., and Ben-Hur, T. (2021). CD200 -dependent and -independent immune-modulatory functions of neural stem cells. Stem Cell Res. *56*, 102559. https://doi.org/10.1016/j.scr.2021.102559.

40. Borst, K., Dumas, A.A., and Prinz, M. (2021). Microglia: immune and non-immune functions. Immunity *54*, 2194–2208. https://doi.org/10.1016/j.immuni.2021.09.014.

41. Zhang, B., Ohtsuka, Y., Fujii, T., Baba, H., Okada, K., Shoji, H., Nagata, S., Shimizu, T., and Yamashiro, Y. (2005). Immunological development of preterm infants in early infancy. Clin. Exp. Immunol. *140*, 92–96. https://doi.org/10.1111/j.1365-2249.2005.02741.x.

42. Berrington, J.E., Barge, D., Fenton, A.C., Cant, A.J., and Spickett, G.P. (2005). Lymphocyte subsets in term and significantly preterm UK infants in the first year of life analysed by single platform flow cytometry. Clin. Exp. Immunol. *140*, 289–292.

43. Rechavi, E., and Somech, R. (2017). Survival of the fetus: fetal B and T cell receptor repertoire development. Semin. Immunopathol. *39*, 577–583. https://doi.org/10.1007/s00281-017-0626-0.

44. Dwyer, J.M., and Mackay, I.R. (1972). The development of antigen-binding lymphocytes in foetal tissues. Immunology *23*, 871–879.

45. Blencowe, H., Lawn, J.E., Vazquez, T., Fielder, A., and Gilbert, C. (2013). Preterm-associated visual impairment and estimates of retinopathy of prematurity at regional and global levels for 2010. Pediatr. Res. *74* (*Suppl 1*), 35–49. https://doi.org/10.1038/pr.2013.205.

46. Wang, C., Luan, Z., Yang, Y., Wang, Z., Wang, Q., Lu, Y., and Du, Q. (2015). High purity of human oligodendrocyte progenitor cells obtained from neural stem cells: suitable for clinical application. J. Neurosci. Methods *240*, 61–66. https://doi.org/10.1016/j.jneumeth.2014.10.017.

47. Schneider, C.A., Rasband, W.S., and Eliceiri, K.W. (2012). NIH Image to ImageJ: 25 years of image analysis. Nat. Methods *9*, 671–675. https://doi.org/10.1038/nmeth.2089.

48. Varga, V.S., Molnár, B., and Virág, T. (2012). Automated high throughput whole slide imaging using area sensors, flash light illumination and solid state light engine. Stud. Health Technol. Inf. *179*, 187–202.

49. Gautier, M.K., and Ginsberg, S.D. (2021). A method for quantification of vesicular compartments within cells using 3D reconstructed confocal z-stacks: comparison of ImageJ and Imaris to count early endosomes within basal forebrain cholinergic neurons. J. Neurosci. Methods *350*, 109038. https://doi.org/10.1016/j.jneumeth.2020.109038.

STAR★METHODS

KEY RESOURCES TABLE

REAGENT or RESOURCE	SOURCE	IDENTIFIER
Antibodies		
Mouse-anti A2B5	R&D Systems	Cat. #MAB1416, RRID: AB_357687
Rabbit-anti PDGF receptor-α	Cell Signaling Technology	Cat. #C5241, RRID: AB_10692773
Rabbit-anti OLIG2	Millipore	Cat. #AB9610, RRID: AB_570666
Mouse-anti SOX10	R&D Systems	Cat. #MAB2864, RRID: AB_2195180
Mouse-anti nestin	Abcam	Cat. #ab6320, RRID: AB_308832
BV421 PDGFR-α mouse anti-human	BD Biosciences	Cat. #562799, RRID: AB_2737804
PE A2B5 mouse anti-human	Miltenyi Biotec	RRID: AB_10830711
PerCP/Cyanine5.5 anti-rat CD45	Biolegend	Cat# 202220; RRID: AB_10683172
PE anti-rat CD3	Biolegend	Cat# 201412; RRID: AB_2563273
APC/Cyanine7 anti-rat CD4	Biolegend	Cat# 201518; RRID: AB_1186084
PE/Cyanine7 anti-rat CD8a	Biolegend	Cat# 201716; RRID: AB_2814100
APC anti-rat CD28	Biolegend	Cat# 200908; RRID: AB_2073971
APC Mouse IgG1, κ Isotype Ctrl	Biolegend	Cat# 400119; RRID: AB_2888687
PE anti-rat CD45RC	Biolegend	Cat# 204007; RRID: AB_1186138
PE Mouse IgG1, κ Isotype Ctrl	Biolegend	Cat# 400112; RRID: AB_2847829
PE anti-rat CD25	Biolegend	Cat# 202105; RRID: AB_314002
Alexa Fluor® 647 anti-mouse/rat/human FOXP3	Biolegend	Cat# 320014; RRID: AB_439750
Alexa Fluor® 647 Mouse IgG1, κ Isotype Ctrl (ICFC)	Biolegend	Cat# 400155; RRID: AB_2832978
PerCP/Cyanine5.5 anti-rat CD45	Biolegend	Cat# 202220; RRID: AB_10683172
PE anti-rat CD3	Biolegend	Cat# 201412; RRID: AB_2563273
APC/Cyanine7 anti-rat CD4	Biolegend	Cat# 201518; RRID: AB_1186084
PE/Cyanine7 anti-rat CD8a	Biolegend	Cat# 201716; RRID: AB_2814100
APC anti-rat CD28	Biolegend	Cat# 200908; RRID: AB_2073971
APC Mouse IgG1, κ Isotype Ctrl	Biolegend	Cat# 400119; RRID: AB_2888687
PE anti-rat CD45RC	Biolegend	Cat# 204007; RRID: AB_1186138
PE Mouse IgG1, κ Isotype Ctrl	Biolegend	Cat# 400112; RRID: AB_2847829
PE anti-rat CD25	Biolegend	Cat# 202105; RRID: AB_314002
Alexa Fluor® 647 anti-mouse/rat/human FOXP3	Biolegend	Cat# 320014; RRID: AB_439750
Alexa Fluor® 647 Mouse IgG1, κ Isotype Ctrl (ICFC)	Biolegend	Cat# 400155; RRID: AB_2832978
mouse-anti CD4	Abcam	Cat. #ab33775, RRID: AB_726468
mouse-anti CD8	Bio-Rad	Cat. #MCA48G, RRID: AB_32147
mouse-anti OX42	Bio-Rad	Cat. #MCA275G, RRID: AB_321301
mouse-anti HNA	Millipore	Cat. #MAB1281, RRID: AB_94090
mouse-anti Stem121	TaKaRa	Cat. #Y40410, RRID: AB_2801314
rat-anti MBP	Bio-Rad	Cat. #MCA409S, RRID: AB_325004
Alexa 488-conjugated donkey anti-mouse	Abcam	Cat. #ab150105, RRID: AB_2732856
Alexa 594-conjugated donkey anti-rabbit	Abcam	Cat. #ab150064, RRID: AB_2734146
Alexa 488-conjugated donkey anti-rabbit	Abcam	Cat. #ab150153, RRID: AB_2737355

(*Continued on next page*)

Continued

REAGENT or RESOURCE	SOURCE	IDENTIFIER
Deposited data		
Raw and analyzed data	This paper	https://data.mendeley.com/datasets/hpshy3gddf/draft?a=4d2b303c-2782-4f88-8daf-403fc9edd4aa
Experimental models: Cell lines		
Human neural stem cells	The pediatrics laboratory of the sixth medical center of the Chinese PLA General Hospital	the China National Institute for Food and Drug Control (SH20220032)
human oligodendrocyte precursor cells	The pediatrics laboratory of the sixth medical center of the Chinese PLA General Hospital	differentiated from hNSCs
Experimental models: Organisms/strains		
Rats: Wistar rats	Beijing Sibeifu Biotechnology Co., Ltd	N/A
Software and algorithms		
ImageJ	Schneider et al.[47]	https://imagej.nih.gov/ij/
3DHISTECH	Viktor Sebestyén Varga et al.[48]	https://www.3dhistech.com/
Imaris software	Megan K Gautier et al.[49]	https://imaris.oxinst.com/
Other		
insulin needles	China Food and Drug Administration	No. 20183140467
nanometer carbon suspension	State Food & Drug Administration of China	No. H20041829
Microliter Syringes	Hamilton	Cat. #87900

RESOURCE AVAILABILITY

Lead contact

Further information and requests for resources and reagents should be directed to and will be fulfilled by the lead contact, Dou Ye (yedou666199@163.com) who is also the point person for technical questions about the protocol.

Materials availability

This study did not generate new unique reagents.

Data and code availability

Raw and analyzed data from Figures 1, 2, 3, 4, 5, 6, 7, and 8, and Figures S1–S5 have been deposited at Mendeley and the DOI is listed in the key resources table. This paper does not report original code. Any additional information required to reanalyze the data reported in this paper is available from the lead contact upon request.

EXPERIMENTAL MODEL AND SUBJECT DETAILS

For experimental animal models

All animal operations were performed approved by the Experimental Animal Welfare and Ethics Committee of Beijing Physical and Chemical Analysis and Testing Center (Ethics number: 210520-SWDWF-003). The animal model we studied is an experimental model of intrauterine desensitization involving female Wistar rats of 15–17 days gestation. During intrauterine desensitization, the fetus is too small to judge whether source fetal material is male or female.

There are few influence (or association) of sex, gender, or both on the results of the study. We recorded the gender of rats that got transplantation after 6 weeks of desensitization:

In the **control** group, because there was no surgical operation for intrauterine desensitization, we included 12 rats (6 males and 6 females) into the control group which littermates of the same sex were randomly assigned to four experimental groups based on the cells of transplantation.

(1) Control_OPC-1: (4 males and 2 females); involving 3 Wistar rats after 10 weeks of desensitization, 3 Wistar rats after 34 weeks of desensitization

(2) Control_NSC-1: (1 males and 2 females);

(3) Control_OPC-2: (2 males and 1 females);

(4) CSA_OPC-1: (1 males and 2 females).

In each intrauterine desensitization group, rats went through the surgery who survived were chosen to each group. These successfully survived rats, we can't control the male and female ratio of these rats. We recorded the gender of rats that got transplantation. Littermates of the same sex were randomly assigned to experimental groups.

In **i.p.**_OPC-1 group included 11 rats (4 males and 7 females), which were assigned to three groups based on the cells of transplantation.

(5) i.p._OPC-1, (4 males and 2 females); involving 3 Wistar rats after 10 weeks of desensitization, 3 Wistar rats after 34 weeks of desensitization;

(6) i.p._NSC-1, (1 males and 1 females);

(7) i.p._OPC-2, (1 males and 2 females).

In **i.p.+brain**_OPC-1 group included 13 rats (5 males and 8 females), which were assigned to three groups.

(8) i.p.+brain_OPC-1, (3 males and 3 females); involving 3 Wistar rats after 10 weeks of desensitization, 4 Wistar rats after 34 weeks of desensitization;

(9) i.p.+brain_NSC-1, (1 males and 2 females);

(10) i.p.+brain_OPC-2, (1 males and 2 females); In **(11) i.p.+muscle**_OPC-1 group included 6 rats (4 males and 2 females); involving 2 Wistar rats after 10 weeks of desensitization, 3 Wistar rats after 34 weeks of desensitization; One Wistar rats died during feeding; In **(12) i.p.+muscle+brain**_OPC-1 group included 9 rats (6 males and 3 females). involving 4 Wistar rats after 10 weeks of desensitization, 3 Wistar rats after 34 weeks of desensitization; Two Wistar rats died during feeding.

The animals in the dividal ventilated Cages (IVC) are raised in an environment of 20–26 °C and 40%–70% humidity. The SPF laboratory is located on the 4th floor of Building B, Incubation Building, No. 7, Fengxian Middle Road, Haidian District, Beijing, China. The food for the animals is purchased from Beijing Sibeifu Biotechnology Co., Ltd. The drinking water from the tap water has been disinfected with softened ozone under high pressure.

For cell lines

hNSCs were prepared in the pediatric laboratory of the Sixth Medical Center of PLA General Hospital, Beijing, China, authenticated by National Institutes for Food and Drug Control of China (Report number: SH20220032). The sex of hNSCs is male. hNSCs have been tested for mycoplasma contamination. hNSCs were cultured in Dulbecco's modified Eagle medium (DMEM) mixed with F12 medium (3:1) supplemented with HEPES, D-glucose, progesterone, putrescine, sodium selenite, insulin, heparin, L-glutamine, basic fibroblast growth factor (bFGF), epidermal growth factor (EGF), leukemia inhibitory factor (LIF), and penicillin and streptomycin. hNSCs were seeded into T25 (2×10^6 cells/bottle), maintained at 37°C in a humidified atmosphere with 8.5% CO_2 in an incubator, passaged every 15 days. hNSCs were digested by 1 mL of accutase into single cells which were re-suspended in hOPCs differentiation medium which contains Neurobasal™-A Medium mixed with putrescine, GlutaMAX™-1, B27, platelet-derived growth factor (PDGF), neurotrophic factor-3 (NT3), bFGF, EGF, LIF, and penicillin and streptomycin, and inoculated on a 6-well platepre-coated with fibronectin human plasma and laminin with 200 000 OPCs /well. Half the medium

of hOPCs was replenished every 3 d. Ten of passage of hNSCs and three to five of passage of hOPCs were chosen to transplanted.

METHOD DETAILS

Preparation of hNSCs and hOPCs for desensitization and transplantation

The hNSCs and hOPCs which derived from hNSCs isolated from the human fetal brain were prepared by the pediatrics laboratory of the sixth medical center of the Chinese People's Liberation Army General Hospital Beijing, China, on September 2019.[46] hNSCs (2×10^6 cells/bottle) were seeded into T25 cell culture bottles in 5 mL of culture media which contains Dulbecco's modified Eagle medium (DMEM) mixed with F12 medium (3:1) supplemented with HEPES, D-glucose, progesterone, putrescine, sodium selenite, insulin, heparin, L-glutamine, basic fibroblast growth factor (bFGF), epidermal growth factor (EGF), leukemia inhibitory factor (LIF), and penicillin and streptomycin at 37 °C in a humidified atmosphere with 5.0% CO_2. hNSCs were digested by 1 mL of Accutase-Enzyme Cell Detachment Medium (Cat. #00-4555-56, Thermo Fisher Scientific, Waltham, Massachusetts, USA) into single cells which were re-suspended in hOPCs differentiation medium which contains Neurobasal™-A Medium mixed with putrescine, GlutaMAX™-1, B27, platelet-derived growth factor (PDGF), neurotrophic factor-3 (NT3), bFGF, EGF, LIF, and penicillin and streptomycin, and inoculated on a 6-well platepre-coated with fibronectin human plasma and laminin with 200 000 OPCs /well. Half the medium of hOPCs was replenished every 3 days. To identify the characteristics of hNSCs and hOPCs, the cells were seeded in 24-well plates and immunofluorescence staining was performed using mouse anti-A2B5 (1:50; Cat. #MAB1416, R&D Systems, Minneapolis, MN, USA, RRID: AB_357687), rabbit anti-platelet-derived growth factor (PDGF) receptor-α (1:800; Cat. #C5241, Cell Signaling Technology, Boston, MA, USA, RRID: AB_10692773), rabbit anti-oligodendrocyte transcription factor 2 (OLIG2) (1:300; Cat. #AB9610, Millipore, MA, USA, RRID: AB_570666), mouse anti-sex-determining region Y (SRY)-box transcription factor 10 (SOX10) (1:300; Cat. #MAB2864, R&D Systems, Minneapolis, MN, USA, RRID: AB_2195180), and mouse anti-nestin (1:100; Cat. #ab6320, Abcam, Cambridge, UK, RRID: AB_308832). Flow cytometric analysis was performed using BV421 PDGFR-α mouse anti-human (Cat. #562799, BD Biosciences, Franklin Lake, NJ, USA, RRID: AB_2737804) and PE A2B5 mouse anti-human (Cat. #130-093-581, Miltenyi Biotec, Bergisch-Gladbach, Germany, RRID: AB_10830711).

hOPCs-1 (cells prepared for desensitization), hNSCs-1 (hOPCs-1 differentiated from hNSCs-1), and hOPCs-2 (hOPCs-1 and hNSCs-1 derived from the same fetus whereas hOPCs-2 derived from the other fetus) were respectively included in our study which were digested and resuspended in saline at 4 °C. Ten of passage of hNSCs and three to five of passage of hOPCs were chosen in intrauterine desensitization and transplantation. Desensitization was performed using 100 000 cells/25 μl/site. Six weeks after desensitization, 200 000 cells/3 μl/site from day seven of cell culture were grafted in transplantation.

Intrauterine desensitization

Wistar rats aged 15–17 days *in utero* were anesthetized using Isoflurane (Cat. #R510, BD Biosciences, Franklin Lake, NJ, USA). We made a transverse incision in the abdomens of the pregnant rats to expose the fetal rats, and gently pulled them one by one to a warm saline gauze. The fetuses of Wistar rats at 15–17 days gestation were injected 100 000 hOPCs-1/ 25 μl into brain, limbs (the left forelimb), and abdomen separately ex utero using insulin needles (33G needles, CFDA Device No. 20183140467, China) and labeled the graft site with nanometer carbon suspension (SFDA, Approval No. H20041829, China). While the fetuses of control without injection for desensitization. After desensitization, the fetuses were gently returned to the abdominal cavity, and the cavity was sutured. Wistar rats at gestational ages of 15–17 days were divided into four groups with desensitization of hOPCs-1 (control (n=15), intraperitoneal [i.p.] (n=11), i.p.+muscle [i.p.m] (n=5), i.p.+brain [i.p.b] (n=13), i.p.+muscle+brain [i.p.mb] (n=7) groups) based on the desensitization sites to explore the difference between no desensitization, central and peripheral desensitization to induced immune tolerance.

Flow cytometric analysis of immune cells in rat peripheral blood

Six-, 10-, and 34-week-old Wistar rats were anesthetized by Isoflurane and fixed. The tail was severed and quickly placed in an Eppendorf tube containing heparin sodium (Cat. #H3149, Sigma-Aldrich, St. Louis, MO, USA), and 1.5–1.8 mL of blood was collected. The following antibodies (key resources table) were added after adding red blood cell lysate (Cat. # 420301, BioLegend, St. Louis, MO, USA), and evenly dividing samples into detection, compensation single dye, and ISO tubes. The scheme for flow cytometric

analysis of peripheral blood was provided in Table 3. These membranal antibodies were incubated for 20 min at 28 °C in the dark. For the incubation of Foxp3, we added True-Nuclear™ 1X Fix Concentrate to tube, and incubate at room temperature in the dark for 60 minutes. After that, the Foxp3 antibody was incubated for 60 min at 28 °C in the dark. The washing buffer (key resources table) was added to each tube and thoroughly mixed. All tubes were analyzed using BD–LSRII (BD Biosciences, Franklin Lake, NJ, USA) and data were analyzed on the Flowjo™10 software (BD Biosciences, Franklin Lake, NJ, USA).

Transplantation

Six weeks after desensitization, the Wistar rats were anesthetized, fixed, and then placed on the rat brain stereotactic locator (Kopf900, RWD, Shenzhen, China). We made an incision on the skin of brain and burned the periosteum of the skull with 2% hydrogen peroxide solution (SFDA Approval No. H12020931, China) to expose and establish the graft site (AP=1.28 mm, L=2.0 mm, V=-2.8 mm). We used a skull drill (Cat. #LGZ-1, KEW, Nanjing, China) to make a small hole in the graft site. We transplanted 200 000 hOPCs-1, hNSCs-1 and hOPCs-1/3 μl into the corpus callosum using Microliter Syringes (5 μl, Cat. #87900, Hamilton, Bonaduz, Switzerland) with round-head glass. The syringe was left *in situ* for 3 min and then gradually and gently withdrawn to avoid pulling out the cells left on the syringe. For other graft sites, including desensitized (the left forelimbs) and un-desensitized (the right hind limbs) muscles, we performed the same operations and labeled them with nanometer carbon suspension (SFDA, Approval No. H20041829, China) as the transplantation site. Concomitantly, the cyclosporine (CSA) group was set up to compare the difference between induction of immune tolerance by intrauterine desensitization and immunosuppressive agents. Three days before transplantation, the six-week-old Wistar rats were given an i.p. injection of cyclosporine (10 mg/kg/day) (Cat. #59787-61-0, GlpBio, California, USA) until one month after transplantation, and then cyclosporine (100 μg/ml) was added to drinking water until the observation time point. If continuous weight loss, redness of the eyelids, and nosebleed damage were found in rats during immunosuppression, cyclosporine was reduced or stopped.

Wistar rats at 15–17 days gestation that were desensitized in the uterus via hOPCs-1 were transplanted via hOPCs-1, hNSCs-1 and hOPCs-2 into the abdomen, brain, and muscles. The above rats were distributed into eleven groups (Table 1) to explore the difference in immune tolerance induced by different grafts.

Immunohistochemical and immunofluorescence staining

Wistar rats aged 10 and 34 weeks were euthanized using Chloral hydrate (Cat. #82128-69-6, Sigma-Aldrich, St. Louis, MO, USA) overdose and perfused with phosphate-buffered saline followed by 4% paraformaldehyde (Cat. #15827, Sigma-Aldrich, St. Louis, MO, USA). The brain and muscles were removed and immersed in 20% sucrose until they sank. The whole brain (from the olfactory bulb to the brain stem) was cut coronally in a 1:10 series at 14 μm, and muscles were cut at an 8 μm thickness. Immunohistochemistry and immunofluorescence staining were performed using the primary antibodies: mouse-anti CD4 (1:100, Cat. #ab33775, Abcam, Cambridge, UK, RRID: AB_726468), mouse-anti CD8 (1:300, Cat. #MCA48G, Bio-Rad, California, USA, RRID: AB_32147), mouse-anti OX42 (1:300, Cat. #MCA275G, Bio-Rad, California, USA, RRID: AB_321301), mouse-anti HNA (1:500, Cat. #MAB1281, Millipore, MA, USA, RRID: AB_94090), mouse-anti Stem121 (1:500, Cat. #Y40410, TaKaRa, Shiga, Japan, RRID: AB_2801314), and rat-anti MBP (1:100, Cat. #MCA409S, Bio-Rad, California, USA, RRID: AB_325004). Alexa 488-conjugated donkey anti-mouse (1:500, Cat. #ab150105, Abcam, Cambridge, UK, RRID: AB_2732856), Alexa 594-conjugated donkey anti-rabbit (1:500, Cat. #ab150064, Abcam, Cambridge, UK, RRID: AB_2734146), and Alexa 488-conjugated donkey anti-rabbit (1:500, Cat. #ab150153, Abcam, Cambridge, UK, RRID: AB_2737355) secondary antibodies were used for immunocytochemistry. Cell nuclei were labeled with 4′,6-diamidino-2-phenylindole (DAPI, 1:20, Cat. #28718-90-3, Sigma-Aldrich, St. Louis, MO, USA). Cells were observed using fluorescence microscopy (IX-70, Olympus Corporation, Tokyo, Japan).

Mixed lymphocyte culture

Thirty-four weeks after desensitization, the spleens of Wistar rats in each group were ground and divided into plasma, lymphocytes, monocytes, platelets, granulocytes, or erythrocytes using lymphocyte separation solution (Ficoll-Paque™ Plus, Cat. #17144002, Cytiva, Montana, USA). Lymphocytes and monocytes were collected and centrifuged to produce peripheral blood mononuclear cells (PBMCs), which were then frozen in liquid nitrogen for subsequent usage. hOPCs-1, hNSCs-1, and hOPCs-2 were inoculated on a 48-well plate treated with coating solution overnight. After one day of culture, mitomycin C (20 μg/

mL, Cat. # R051186, RHAWN, Shanghai, China) was used to inactivate the hOPCs and hNSCs. Similarly, PBMCs isolated from the spleen were resuscitated and treated with 5-(and 6)-Carboxyfluorescein diacetate succinimidyl ester (CFSE, 0.1 μM, Cat. #423801, Biolegend, San Diego, California, USA) to assess cell division and proliferation, and were set up without CFSE in the experiment to show that the staining intensity of CFSE was moderate, and were stimulated with concanavalin A (ConA, 5 μl/ml, Cat. #C5275 Magi Sigma, Darmstadt, Germany). The treated PBMCs were seeded into hOPC culture plates (PBMC: hOPC/hNSCs, 5:1) and placed at 37 °C in a humidified 5% carbon dioxide incubator. After three days of mixed lymphocyte culture, each well of the 48-well plate was supplemented with 250 μl of 1640 medium (Cat. #A10491-01, Gibco, Grand Island, New York, USA), and the cells were collected after five days of mixed culture for flow cytometric analysis. The operation steps were the same as above.

QUANTIFICATION AND STATISTICAL ANALYSIS

Quantification of graft cells

We made continuous frozen sections (14 μm/section) of the whole brain (from the olfactory bulb to the brain stem), and collected 1-in-10 sections which were involved 50 to 80 sections for every brain for HNA immunohistochemical staining and counted the number of HNA positive cells. Pannoramic Scan (3D HISTECH) was used to scan a series of coronal sections. For the number of the grafts stained for HNA and optical density (OD) of T-helper cells and microglia were quantified using the ImageJ software (Version 9.8, Bitplane, Zurich, Switzerland). The images were analyzed by setting the quantity threshold, the sum of area, and integrated OD. The number of HNA^+ cells was automatically counted by the Imaris software. All transplanted cells from each brain sample were analyzed under high magnification ($n \geq 3$).

Statistical analysis

Every individual in the chosen samples in the the control group and groups undergoing intrauterine desensitization should be included with an equal chance. The data in this study were analyzed using the GraphPad Prism version 8 software (GraphPad Software, San Diego, CA, USA, www.graphpad.com). All Measurement data are expressed as $x \pm$ STDEV.P. We used SPSS software (26.0) to perform normality test and variance homogeneity test on the samples. Two samples that met the above conditions were subjected to independent sample Student'st-tests, and those that did not meet the above two conditions were subjected to one-way analysis of variance (ANOVA) test; For three samples, when they met the homogeneity of variances, use the LSD test for post hoc multiple comparison, and if they did not meet the homogeneity of variances test, they were subjected to the Tamhini test. Differences were considered statistically significant when $p<0.05$, and $p<0.01$.